ANL-6808
Reactor Technology
(TID-4500, 24th Ed.)
AEC Research and
Development Report

ARGONNE NATIONAL LABORATORY
9700 South Cass Avenue
Argonne, Illinois 60440

REACTOR DEVELOPMENT PROGRAM PROGRESS REPORT

November 1963

Albert V. Crewe, Laboratory Director
Stephen Lawroski, Associate Laboratory Director

Division	Director
Chemical Engineering	R. C. Vogel
Idaho	M. Novick
Metallurgy	F. G. Foote
Reactor Engineering	L. J. Koch
Reactor Physics	R. Avery
Remote Control	R. C. Goertz

Report coordinated by
R. M. Adams and A. Glassner

Issued December 15, 1963

Operated by The University of Chicago
under
Contract W-31-109-eng-38
with the
U. S. Atomic Energy Commission

DISCLAIMER

FOREWORD

The Reactor Development Program Progress Report, issued monthly, is intended to be a means of reporting those items of significant technical progress which have occurred in both the specific reactor projects and the general engineering research and development programs. The report is organized in a way which, it is hoped, gives the clearest, most logical over-all view of progress. The budget classification is followed only in broad outline, and no attempt is made to report separately on each sub-activity number. Further, since the intent is to report only items of significant progress, not all activities are reported each month. In order to issue this report as soon as possible after the end of the month editorial work must necessarily be limited. Also, since this is an informal progress report, the results and data presented should be understood to be preliminary and subject to change unless otherwise stated.

The issuance of these reports is not intended to constitute publication in any sense of the word. Final results either will be submitted for publication in regular professional journals or will be published in the form of ANL topical reports.

The last six reports issued in this series are:

May 1963	ANL-6739
June 1963	ANL-6749
July 1963	ANL-6764
August 1963	ANL-6780
September 1963	ANL-6784
October 1963	ANL-6801

TABLE OF CONTENTS

TABLE OF CONTENTS

TABLE OF CONTENTS

I. BOILING WATER REACTORS

A. BORAX-V

1. Operations

After replacing the leaking fuel assembly C-3 by a spare superheater fuel assembly in central superheater core CSH-1B (see Progress Report for October 1963, ANL-6801, p. 3), the reactor was prepared for resumption of power operation.

A second heat-up of the system, using electric preheaters, was performed in an attempt to reproduce conditions which had caused a short-period scram during the hot critical experiments with superheater drained. The postulated cause, flooding the superheater with condensate from the external steam lines, could not be verified.

Element C-3 was shipped to Argonne, Illinois, for hot cell examination. When the results of the inspection (see Sect. I.A.3 below) were received, reactor operation was curtailed, pending inspection of the remaining superheater fuel. The reactor vessel head was removed, and six superheater fuel assemblies were transferred to superheater fuel storage. Preparations are being made for underwater inspection of the bottom of the fuel plates in these assemblies. Three special underwater periscopes with attached lights have been designed and built in an attempt to inspect the lower end of the superheater fuel plates visually.

2. Modification and Maintenance

As a result of the information derived from the hot cell examination of defective superheater fuel assembly C-3 (see Sect. I.A.3 below), the bottom nozzles of the three spare superheater fuel assemblies are being removed. All burned-through repair weld material is being removed to restore the designed expansion capability of the 4-plate fuel elements relative to the insulating tube. The bottom nozzles will be replaced and the fuel assemblies straightened and leak-tested.

3. Hot Cell Examination of Damaged Superheater Fuel Assembly C-3

The central section of the damaged superheater fuel assembly C-3 was cut out. This consists of five fuel subassemblies. The fuel subassemblies, which consist of a brazed assembly of four fuel plates (the fuel-plate subassembly) surrounded by an insulating can, were separated. These cans were subsequently removed. In addition, a number of lateral cuts were made through two of the fuel plate subassemblies.

External damage in the form of bulged insulating cans, bowed fuel plate subassemblies, and a crack in the transition cone was observed. Two of the fuel-plate subassemblies were buckled, nearly blocking the passages for steam flow. In the other three, a number of individual fuel plates were bent and two appeared to be torn. In all of the fuel subassemblies, there was partial fusion of the lower ends of the two outer fuel plates to the surrounding insulating can. In two subassemblies, at least 50 percent of the circumference of the insulating cans was firmly fused to the adjacent fuel plates. In the other subassemblies there were a number of short fused areas. In the two firmly fused subassemblies, all four fuel plates were buckled. In the subassemblies with short fused areas, buckling occurred only in the individual fuel plate adjacent to the fused area.

In the BORAX-V superheater fuel assembly, the lower end of each fuel plate subassembly is free to move with respect to its insulating can to allow for thermal expansion. In the case of superheater fuel assembly No. C-3 the observed fusion of the free ends of the fuel plates to the insulating can prevented this motion. It is believed that the differential thermal expansion and contraction during reactor operation was sufficient to cause the observed damage. For example, the bulges in the insulating cans could result from the stretching of the cans upon heating and subsequent buckling of the cans upon cooling.

Fusion of the fuel plates to the insulating cans probably occurred during repair welding (see Progress Report for September, ANL-6789, p. 1). During this repair operation it was intended to weld only the insulating cans to flow vanes between the adjacent cans. The weld burn-through restrained the 4-plate fuel element from expanding as designed in both the transverse and longitudinal direction, thus causing severe fuel-plate distortion at the bottom and buckling of the element at the axial high neutron flux region. The fission product release was not caused by a design error or material selection, but by faulty repair and inspection procedures. A possibility that this fusion could have occurred during reactor operation is unlikely, since the fused area is not in the fueled part of the plate.

4. Development of In-core Instrumentation

A test report of furnace calibration of six high-temperature W/26% Re-sheathed thermocouples was received from a commercial testing agency (see Progress Report for September 1963, ANL-6784, p. 4). These W/5% Re versus W/26% Re couples utilized hard-fired, high-purity thoria insulators in 0.065-in.-OD sheaths.

The test was conducted in two sections, with three samples being grouped for testing each time. Two cycles, to maximum temperature (5000°F, nominal), were made for each group of thermocouples, with 15-20 min allowed for stabilization before each reading. The thermocouples

were installed in a tantalum tube within the graphite heating element of the furnace and were blanketed with high-purity argon. The optical pyrometer system was calibrated by determination of molybdenum and platinum melting points in the same furnace configuration as used for calibration of the thermocouples.

Data are shown graphically for the two test groups in Figures 1 and 2. The second-cycle data in Figure 2 are not consistent with those of Figure 1. The only explanation given by the test agency is that their furnace required shutdown and repair after running the first cycle on samples 30, 31 and 32. It was postulated that the samples were somehow subjected to

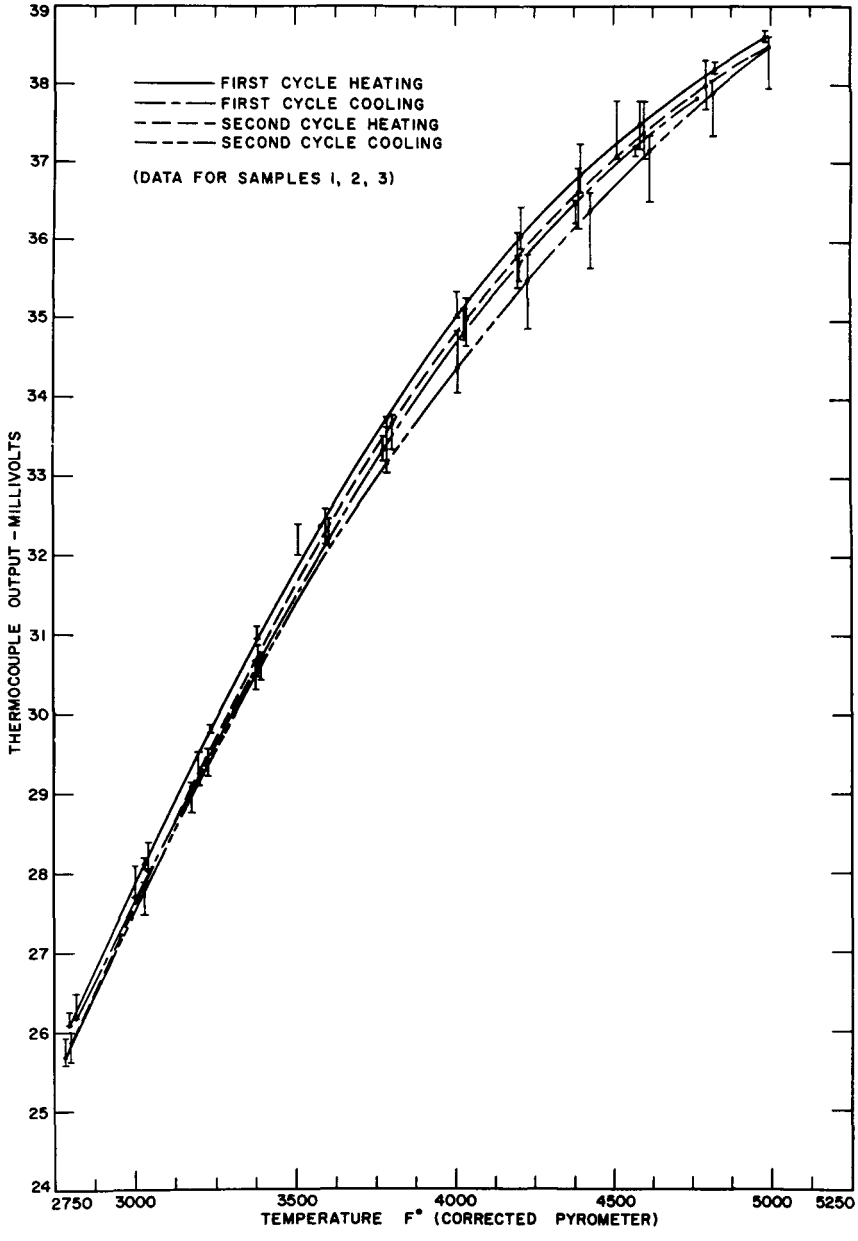

Figure 1. Calibration of W-5% Re vs. W-26% Re Thermocouples (Samples 1, 2, and 3) in Argon Atmosphere

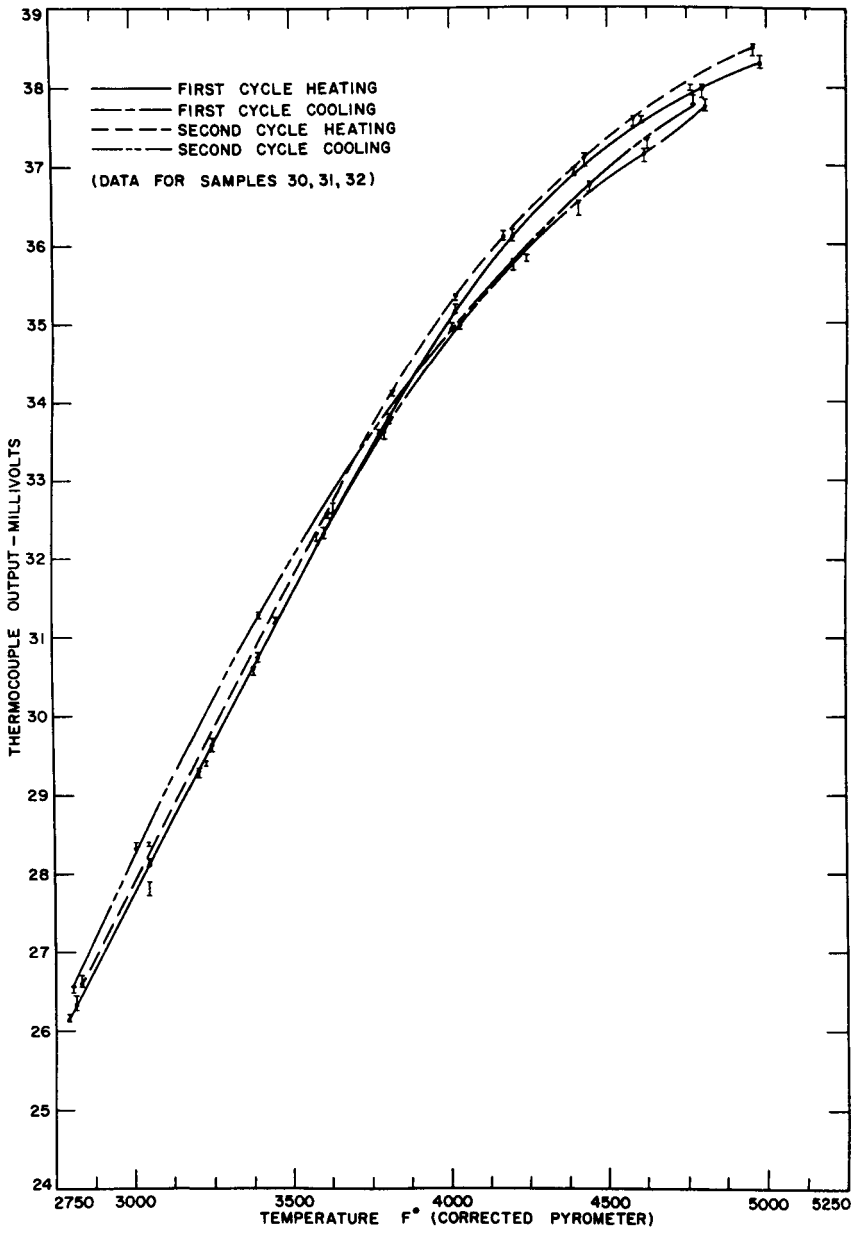

Figure 2. Calibration of W-5% Re vs. W-26% Re Thermocouples (Samples 30, 31, and 32) in Argon Atmosphere

different conditions for the second furnace cycle, although the axial temperature gradient in the region near the hot junctions of the couples is only about 20°F/in. This factor alone does not explain the discrepancy.

5. Development of Advanced Superheater Fuel

a. Type 406 Stainless-clad Superheat Fuel. The fuel plates to be used in two central superheat fuel elements (see Progress Report for January 1963, ANL-6683, p. 5) have been nickel plated for brazing to the cladding. Thermocouple pockets have to be machined into the edges of the plates before further assembly. The choice of alloy to be used for brazing the four-plate fuel subassemblies has not yet been made.

II. LIQUID-METAL-COOLED REACTORS

A. General Fast Reactor Physics

1. ZPR-III

The program of preliminary experiments with the physics core for the mock-up of RAPSODIE was completed. These included evaluation of the reactivity shutdown provided by all the safety rods, calibration of control rods, calibration of BF_3 and fission chamber count rates versus subcriticality for reactivity measurements, and measurements of dead time of the BF_3 proportional counters for reactivity measurements. The scaler strips of the proportional counter channels provide the principal amount of dead time, amounting to about 6 to 8 μsec. These dead times will be used to adjust the data taken in period measurements and power level determinations.

A one-inch withdrawal of a central safety rod, which is a core drawer on the reactor axis, was found to decrease reactivity by about 72 Ih. This is to be compared with worths of 50 Ih for a core-loaded rod at the radial edge of the core and 17 Ih for a blanket-loaded rod at the core radial edge for the same withdrawal. On the basis of these values and the control rod calibrations, the total shutdown margin is estimated at about 3100 Ih, or about 6%Δk/k, minus about 200 Ih excess used for operation.

Measurements of fission ratios at the core center are in progress. The central core drawer in Half No. 1 of the reactor is constructed to accommodate a sole Kirn-type fission chamber at the front. Count rates with this chamber are then established relative to the BF_3 proportional counters and to a Kirn U^{235} counter at the core axial edge. Kirn chambers containing U^{233}, U^{234}, U^{235}, U^{236}, U^{238}, Pu^{239}, and Pu^{240} as the principal isotopes will all be run at the center. Additional measurements with thin-wall, gas-flow chambers will be made for the threshold fission isotopes.

2. ZPR-VI

Assembly No. 1, an all-metal assembly with a U^{238}/U^{235} atom ratio of about 7, is being used to measure various reactor physics parameters. Bunching experiments to determine the heterogeneity effect of the fuel plates are currently in progress.

The following fission ratios have been obtained by means of miniature solid-state detectors:

$$U^{238}/U^{235} = 0.0395 \pm 0.0015; \qquad U^{233}/U^{235} = 1.625 \pm 0.008.$$

These results correspond to the values of 0.036 and 1.51 found, respectively, for the same fission ratios obtained by gas-flow detectors in Assembly 11 of the ZPR-III facility, which is very much like Assembly 1 of ZPR-VI.

A number of gap-worth measurements were made with Assembly 1. Measurements were made with air and stainless steel in the gap. The results are shown in Figure 3. A point to be noted is that at zero separation and at zero reactivity change, which corresponds to the situation when the drawer faces of both halves are touching, there is still a separation of the fuel of the two halves due to the thickness of the stainless steel drawer ends.

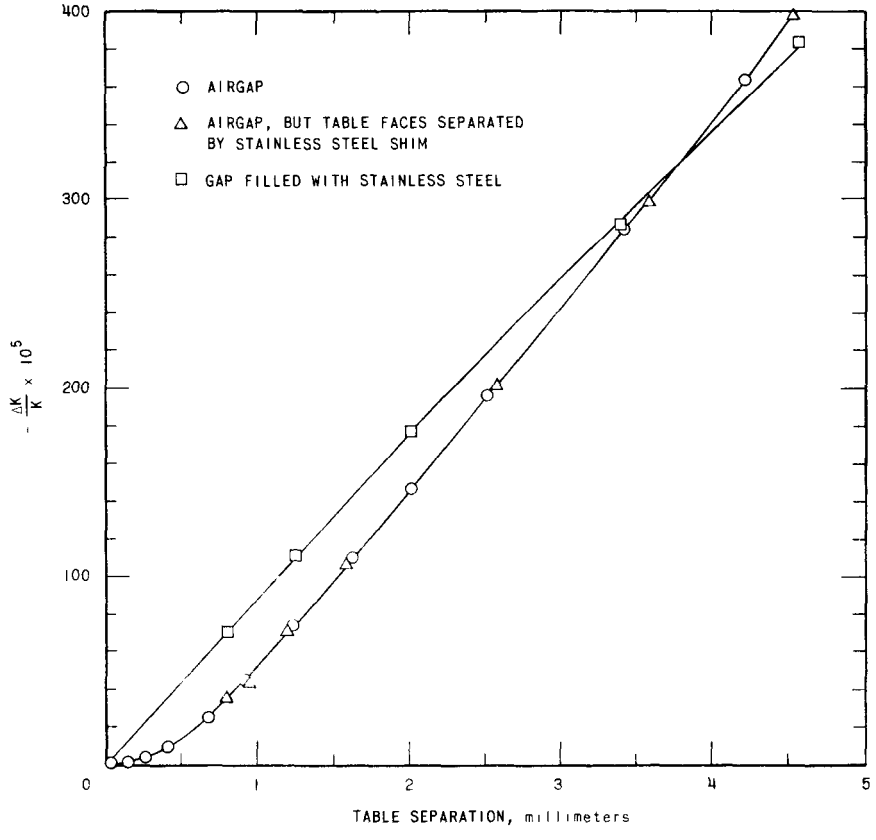

Fig. 3. The Reactivity Calibration Curve for the Gap for Assembly 1 of ZPR-VI

It is noted that with an air gap less than 0.5 mm, the slope of the reactivity curve is substantially less than for an air gap greater than 0.5 mm. An attempt was made to determine whether this was due to a slight tilting of the matrix assembly due to the nonparallel bearing faces of the bed. A 0.80-mm shim was inserted between the table faces and the air gap worth was remeasured. If the change in slope is due to the tilting of the matrix caused by nonparallel bearing surfaces, it would be expected that the slope would be translated to the right by the thickness of the shim (0.80 mm). The data do not indicate such an effect.

A possible explanation of the change in slope of the reactivity table separation curve is that the surfaces of the reactor halves are not plane parallel. A theoretical prediction for this effect has not yet been performed.

It is noted that the reactivity-separation curve for the stainless steel-filled gap appears to be linear for small gaps and has a different slope. The curves for the air gap and stainless steel-filled gap cross between 3.5 and 4.0 mm of gap width. There appears to be an erroneous data point in the stainless steel curve which results in some uncertainty in the crossover point. Examination of the data does not reveal the suspect point; however, in general the characteristics of the two gap-separation curves are well displayed.

3. ZPR-IX

The aluminum tube bundles sent out for coating have been returned. All have been stacked and precisely aligned to form the complete matrix assembly. Each individual tube has been stamped with identifying numerals to denote its position in the matrix.

The coated matrix drawers have been received from the vendor and have been stamped with identifying numerals corresponding to the position of the tube to which they will be assigned.

The final checkout of the facility as a complete system, including the mechanical and electrical components and nuclear instrumentation, is currently in progress.

B. General Fast Reactor Fuel Development

1. Metal Fuels

a. Properties of U-Pu-Fz. The effects of the variables of heat treatment and specimen position in the casting on the mechanical properties measurements of U-Pu-Fz alloys have been studied. The top and bottom of the 40.5-cm (16-in.) long by 1-cm (0.4-in.) diameter injection casting were given a homogenizing heat treatment prior to tensile testing. At 655°C specimens from both the top and the bottom had about the same strength (6,000 psi), but the elongation of the top was 22.5% compared with 31.3% for the bottom.

The two specimens from the center of the casting were tested at room temperature, one in the quenched condition and the other in a transformed state corresponding to a 20-hr anneal at 500°C. Both were extremely brittle, with elongations of less than 1%. The quenched specimen had a strength of 84,000 psi whereas the transformed one broke outside the gauge length at a much lower value. The transformed phase is so brittle and notch sensitive that its true strength cannot be measured with this tensile-testing technique.

U-Pu and U-Pu-Fz alloys are being tested for compatibility with potential refractory cladding metals to help in the selection of a fuel and cladding material for a possible second generation core for EBR-II. The fuel-cladding combinations that are being studied are U-10 w/o Pu and U-20 w/o Pu-10 w/o Fz with niobium, and U-10 w/o Pu-10 w/o Fz with niobium, Nb-1 w/o Zr, molybdenum, vanadium, V-10 w/o Ti, V-20 w/o Ti, Type 304 stainless steel, and Hastelloy-X. These combinations are being studied by annealing diffusion couples of the materials at 550, 600, and 650°C for 7, 17, and 42 days.

Preliminary results of compatibility of U-10 w/o Pu-10 w/o Fz with Hastelloy-X at 600 and 650°C have been obtained. Owing to etching difficulties with U-Pu-Fz we have been unable as yet to bring out a satisfactory diffusion band on the fuel side of the couple. There are, however, indications that a wide band is present in the fuel of these couples. These bands in the fuel indicate that the majority of the penetration is into the fuel. We experienced the same difficulty in the Type 304 stainless steel versus U-10 w/o Pu-10 w/o Fz. A comparison of the diffusion penetration of this fuel into Hastelloy-X and Type 304 stainless steel (see Table I) indicates that Type 304 stainless steel suffers only about one-half the penetration by the fuel that Hastelloy-X does.

Table I. Penetration of U-10 w/o Pu-10 w/o Fz into Hastelloy-X and Type 304 Stainless Steel

	Penetration (μ)			
	17 days		42 days	
Temp (°C)	Hastelloy-X	304 SS	Hastelloy-X	304 SS
600	10	7	18	10
650		16	39	22

2. Fuel Jacket Development

a. Alloy Development. The Nb-10 w/o Ti mentioned in the September Progress Report (ANL-6784, p. 12) was heat treated for 2 hr at 850°C in vacuo and then cold rolled 50% to a thickness of 0.8 mm (0.031 in.). A Nb-15 w/o Ti-6 w/o V alloy which was previously hot worked was cold reduced approximately 50% to 1.6 mm (0.062 in.) and is now awaiting heat treatment before final rolling.

b. Duplex Tubing. The Type 304 stainless steel-vanadium duplex tube mentioned in the October Progress Report (ANL-6801, p. 12) was checked by ultrasonics after ironing. Nonbonding was detected in approximately 50% of the bond-contact area, presumably a direct result of the

prior ironing operation. The duplex tube was annealed at 850°C for 2 hr in vacuum and ultrasonically tested again. The nonbond area seemed to diminish slightly. The tube was then ironed and reduced to 0.919-cm (0.362-in.) O.D. x 0.792-cm (0.312-in.) I.D., yielding a D/t ratio of 14.5; suitable for ductile core (copper) drawing to approximately 0.396-cm (0.156-in.) I.D. x 0.0381-cm (0.015-in.) wall. The ductile-core drawing is in process.

c. V-10 w/o Ti (TV-10) and V-20 w/o Ti (TV-20) Alloys. The 1110°C extruded TV-10 and TV-20 material has been dejacketed by machining. The rods showed severe longitudinal striations along the total extruded length in addition to the nonuniform diameter previously mentioned in the October Progress Report (ANL-6801, p. 12). The as-extruded hardness of the TV-10 alloy measured about 186 DPH (89 R_B); that of the TV-20 alloy was about 233 DPH (98 R_B). For comparison, hardness readings of Type 304 stainless steel extruded at 1100°C measured 137-139 DPH (74 R_B).

Metallographic examination of the "as-extruded" material revealed a fine-grained structure essentially completely recrystallized. Heat treatment of the "as-extruded" material showed gross grain growth accompanied by a minor decrease in hardness after one hour at 1200°C.

No difficulties have been experienced in cold working either of these alloys.

3. Corrosion of Fuel-cladding Materials

A group of five niobium-base alloys in two conditions of heat treatment has been tested in flowing (15 cm/sec) sodium for 150 hr at 650°C. Zirconium turnings in the sodium stream were used to getter oxygen during exposure of the samples. The oxygen content of the sodium was 120 ppm.

The alloys tested and pre-exposure heat treatments are listed in Table II.

Table II. Compositions and Heat Treatments of Corrosion-test Specimens

Alloy*	Stress-relief Temperature, °C**	Recrystallization Temperature, °C**
Nb-5 Mo	800	1100
Nb-10 Ti-5 Zr	600	1100
Nb-18 Ti-4 V	600	1050
Nb-3 Mo-9 Ti	600	1100
Nb-10 W-2.5 Zr	950	1250

*Compositions given in weight percent.

**Heat treated at indicated temperature in evacuated (10^{-6} torr) capsules for 2 hr.

The weight and thickness change data are summarized in Table III.

Table III. Corrosion of Niobium-base Alloys in Flowing Sodium

Alloy**	Rate of Weight Loss, $mg/cm^2/mo$*
Nb-5 Mo (SR)†	55.6
Nb-5 Mo (RX)	43.4
Nb-10 Ti-5 Zr (SR)	17.1
Nb-10 Ti-5 Zr (RX)	80.7
Nb-18 Ti-4 V (SR)	50.6
Nb-18 Ti-4 V	66.0
Nb-3 Mo-9 Ti (SR)	72.8
Nb-3 Mo-9 Ti (RX)	63.7
Nb-10 W-2.5 Zr (SR)	13.1
Nb-10 W-2.5 Zr (RX)	38.6

*Cleaned of sodium with alcohol and water. Nonadherent oxide removed with soft brush.

**Compositions given in weight percent.

†(SR) - Stress Relieved;
(RX) - Recrystallized.

All samples showed varying degrees of intergranular attack. The most extreme example was that of the Nb-10 w/o W-2.5 w/o Zr (RX) sample. The intergranular attack of the stress-relieved samples (which exhibited highly worked structures) occurred along the smeared-out grain boundaries. The recrystallized samples were attacked along the equiaxed grain boundaries.

There is a very large difference in weight loss between stress-relieved Nb-10 w/o Ti-5 w/o Zr and Nb-10 w/o W-2.5 w/o Zr alloys and recrystallized alloys of the same composition. From metallographic evidence it is believed that the grain boundaries of the recrystallized samples were completely corroded away, resulting in the physical loss of complete grains. However, it should be noted that the effect of the recrystallizing heat treatment is not uniformly severe for all alloys tested.

Microhardness measurements taken across the transverse sections of the samples showed varying profiles, ranging from a constant hardness increase in the case of the Nb-5 w/o Mo samples (similar to the behavior of this material in low-oxygen sodium) to very steep hardness gradients at

the surface (approximately 100-150μ thick) for the Nb-10 w/o Ti-5 w/o Zr, Nb-18 w/o Ti-4 w/o V, and Nb-3 w/o Mo-9 w/o Ti samples. The Nb-10 w/o W-2.5 w/o Zr alloy showed a much more shallow hardness gradient from edge to center. There were no distinct differences between the hardness profiles of the stress-relieved and recrystallized samples.

An additional group of alloys has been tested for 216 hr under the same conditions as the previous group. A detailed metallographic examination is in progress. The preliminary weight change data are listed in Table IV. The rates of weight loss of the vanadium-base alloys are less by more than an order of magnitude than those for niobium-base materials tested under the same conditions.

Table IV. Corrosion of Vanadium-Titanium Alloys and of Niobium in Flowing Sodium

Alloy**	Rate of Weight Loss, mg/cm^2/mo*	Alloy**	Rate of Weight Loss, mg/cm^2/mo*
V-10 Ti (SR)†	3.23	V-20 Ti (RX)†	3.72
V-10 Ti (RX)	2.76	Nb (SR)	41.6
V-20 Ti (SR)	3.33	Nb (RX)	52.8

*Cleaned of sodium with alcohol and water. Nonadherent oxide removed with brush.
**Compositions given in weight percent.
†(SR) - Stress Relieved; (RX) - Recrystallized.

4. Nondestructive Tests of Fast Reactor Tubing

Electromagnetic tests on tubing being used or produced for general fast reactor fuel development and the results of these tests are summarized in Table V.

Table V. Electromagnetic Tests on Tubing for Fast Reactor Development

Material	Dimensions	Quantity (m)	Results
D-43*	6.6-mm O.D.	1.3	No defects detected
Hastelloy-X	7.14-mm O.D. x 0.38-mm wall	10.98	No defects detected
Nb-1 w/o Zr	3.96-mm I.D. x 0.508-mm wall	30.5	10 defects >10%
Nb-1 w/o Zr	3.96-mm I.D. x 0.381-mm wall	20.3	7 defects ≥10%
Nb-1 w/o Zr	7.14-mm O.D. x 0.305-mm wall	1.5	1 defect
304 SS	4.21-mm I.D. x 0.508-mm wall	34	2 defects ≥10%
304 SS	4.21-mm I.D. x 0.381-mm wall	39	No defects detected

*Nb-10 w/o W-1 w/o Zr-0.1 w/o C

Radiographic tests on tubing for fast reactor development are listed in Table VI. The inner surfaces of the last four tubes listed in Table VI contained a vapor-deposited tungsten layer of varying thickness. The defects found in these tubes were tungsten inclusions, deep striations and in some instances flaking of the tungsten coating.

Table VI Radiographic Tests on Tubing for Fast Reactor Development

Material	Dimensions	Quantity (m)	Results
Nb-1 w/o Zr (Heat No. 70302)	3.96-mm I.D. x 0 38-mm wall	20.31	Inclusion <10% in 1 tube
Nb-1 w/o Zr (Heat No. 70086)	3.96-mm I.D. x 0.508-mm wall	10.15	No defects
Nb-1 w/o Zr (Heat No. 30305)	3.96-mm I.D. x 0.508-mm wall	10.15	No defects
Nb-1 w/o Zr (Heat No. 30018)	3.96-mm I D. x 0.508-mm wall	10.15	No defects
Hastelloy	7.14-mm O.D. x 0.38-mm wall	10.98	No defects
Hastelloy	4.21-mm I.D x 0.254-mm wall	21 9	6.21 m defective, 0.091-mm to 0.165-mm variation in thickness of tungsten deposit on inner wall
Hastelloy	4.21-mm I.D. x 0.38-mm wall	2.44	No defects, 0.147-mm to 0.172-mm variation in thickness of tungsten deposit on inner wall
Hastelloy	4.21-mm I.D. x 0.508-mm wall	3.66	0 588 m defective, 0.124-mm to 0.170-mm variation in thickness of tungsten deposit on inner wall
Zr-2	5.59-mm O.D. x 0.508-mm wall	0.91	Crack in 1 tube
Zr-2	6.09-mm O.D x 0.508-mm wall	1.68	Low density inclusions in 2 tubes
Zr-2	3.96-mm O.D x 0.408-mm wall	1.22	Numerous cracks noted
304 SS	4.21-mm I.D. x 0.38-mm wall	19.5	1.96 m defective, 0.099-mm to 0.157-mm variation in thickness of tungsten deposit on inner wall

The results of ultrasonic tests on tubing for reactor development are given in Table VII.

Table VII. Ultrasonic Tests on Tubing for Fast Reactor Development

Material	Dimensions	Quantity	Results
304 SS-jacketed vanadium tubing	1 04-cm O.D. x 0.85-cm I.D	1 piece	Incomplete and variable mechanical bond
Hastelloy-X tubing	1.27-cm O.D. x 0.10-cm wall	6 pieces	2 longitudinal O.D seams
Zircaloy-2 duplex tubing	3.73-cm O.D. x 3.12-cm I.D.	2 pieces	Variable mechanical bond but comparable to an acceptable standard
Vanadium rods 10 w/o Ti and V-20 w/o Ti	0.75-cm to 1.09-cm O.D.	163 cm	No transverse or longitudinal defects
Nb-5 w/o V-1.5 w/o Zr Nb-10 w/o W-2.5 w/o Zr Nb-33 w/o Ta-10 w/o W-1 w/o Zr	1.27-cm O.D 1 40-cm O.D. 1.40-cm O D.	92 cm	Longitudinal defect signals. Radiography revealed high-density slivers (probably tungsten)

C. EBR-I, Mark IV

1. Experiments

Experiments were begun to determine the effect of the core tightening and clamping devices on the reactivity changes observed with different modes of operation. Initially, the tightening rods in the seven core subassemblies were loosened, and the reactivity loss after operating at high power and low inlet temperature was measured as 40 Ih. This loss was regained, however, at high inlet temperature. The cycle was repeated four times with consistent results and was the same as the change observed when the tightening rods were fully tightened (high power, low and high inlet temperatures).

The seal plate shoes (six shoes around the full periphery of the outer subassemblies which limit bypass leakage) were loosened one turn. This decreased the flow through the core about 10%, due to increased bypass. To comply with the restriction on the maximum fuel rod temperature, it was necessary to reduce power from 970 to 930 kW. The reactivity changes observed between operation at high and low inlet temperatures decreased to about 20 Ih, or one-half that observed before the seal plate shoes were loosened. This measurement was consistent over five cycles after an initial reactivity loss of about 10 Ih. The seal plate shoes have now been retightened, and the reactivity changes will be observed to see if they return to the former magnitude.

One suggested mechanism for the reactivity loss associated with loosening of the seal plate shoes is a slight separation of the fuel slugs in the jackets due to thermal differential expansion while at power. Physical and X-ray examination of three nonirradiated rods showed the slugs to be perfectly free to move in the jacket as the rods were turned. Postirradiation examination of prototype rods irradiated in Mark III to about 0.1%

burnup showed no physical changes, such as surface roughening or bowing, that would cause the slugs to hang up inside the jacket. The prototype rods were nearly the same alloy composition as the Mark IV rods, but were 8 in. long compared with the four $2\frac{1}{16}$-in. slugs in Mark IV fuel rods.

2. Breeding Gain Measurements

Breeding gain measurements in EBR-I, Mark IV have been completed. Patterns of the Pu^{239} fission were established throughout the core from measurements of the fission product activity generated in aluminum-clad foils of metallic plutonium. In a similar manner, fission patterns for U^{235} and U^{238} in the various blankets were established from measurements of the fission product activity induced in enriched and depleted uranium foils, respectively. Capture profiles for U^{238} were based on observations of the 106-keV Np^{239} photopeak with a NaI crystal gamma spectrometer. In each set of traverse measurements (eight in all), the activity of each foil was measured relative to the activity of a monitor foil which, in turn, was irradiated simultaneously at a fixed reproducible monitoring location. To establish a reliable common base between the various runs, radiochemical analyses were conducted on monitor foils which were irradiated simultaneously at their respective positions.

The various profiles for fission and capture were integrated both radially and axially throughout the core and breeding blankets. Conversion of relative to absolute units through the radiochemical analyses resulted in the fission-capture breakdown summarized in Table VIII.

Table VIII. Summary of Fissions and Captures in EBR-I, Mark IV

Isotopic Species	Fissions x 10^{-18}	Captures x 10^{-18}
U^{235}	0.1429	0.0362
U^{238}	0.206	1.492
Pu^{239}	0.9146	0.0841
Pu^{240}	0.0259	0.0055
Pu^{241}	0.0054	0.0005

Estimates of the fissions and captures in Pu^{240} and Pu^{241} were obtained from the total number of fissions in the plutonium monitor foil (from radiochemical analyses) and effective cross-section values established by multigroup methods. Values for capture in U^{235} and Pu^{239} were

estimated from the fission results and from values established for α_{25} and α_{49} in the EBR-I core by Kafalas et al.[1]

The breeding ratio is defined as

$$BR = \frac{\text{Production of } Pu^{239} \text{ and } Pu^{241}}{\text{Destruction of } U^{235}, Pu^{239}, \text{ and } Pu^{249}}.$$

Substitution of values from Table VIII into this equation results in a breeding ratio of 1.27 ± 0.08, where the precision limits consider uncertainties inherent in the activity measurements, fission and capture integrations, and the radiochemical analyses.

The fast fission bonus, defined as the ratio of the number of fissions in fertile material to the number of absorptions in fissionable material, was evaluated from the information of Table VIII as 0.20 ± 0.02.

D. EBR-II

1. Reactor Plant

a. Criticality. Loading of the reactor for the approach to wet critical was started on October 30, 1963, with the transfer of 17 enriched uranium subassemblies from the storage basket to the reactor grid. Subsequent loadings in increments of 6, 6, 6, 6, 5, 4, 3, and 3 enricheduranium subassemblies were made for a total of 70 subassemblies (including the 12 control and 2 safety rods). The loading continued without major malfunctions for 12 days. Criticality was achieved on November 11, 1963, when the reactor was loaded with 184.3 kg of U^{235} and was supercritical by approximately 163 Ih (0.39% $\Delta k/k$). Subsequent measurements give the clean critical mass to be 181.2 kg U^{235} at 600°F.

The loading was then rearranged to reduce the source strength by a factor of 8 and to make the loading more symmetrical. The new source gave counts on the start-up channels 1, 2, and 3 slightly in excess of 5 counts/sec with control and safety rods down.

b. Preliminary Power Calibration. A preliminary calibration of the instruments was made by irradiating U^{235} foils at the blanket-core interface for a given length of time and at a given instrument reading level. These foils were analyzed radiochemically for total U^{235} fission. By using the calculated fission rate distribution curves, it should be possible to estimate the total integrated power of the reactor to within about 20%. The foil analysis was done both at Chicago and Idaho, and, at present, there is a discrepancy between the two results by a factor of 0.7. The cause for this disagreement is being investigated. A second foil calibration was

[1] P. Kafalas et al., Determination of the Ratio of Capture to Fission Cross Sections in EBR-I, Nuclear Sci. and Eng., 2, 657 (1957).

made at 460°F in order to determine whether there is any change in instrument response as a function of temperature.

c. Control Rod Calibration. Two control rods, No. 7 on a corner and No. 2 on a flat, were calibrated from 0 to 14 in. by period measurements. The total worth of each of the other rods was then measured by comparison with these. Intercomparisons were always made between rods across the core from each other. Table IX gives the individual worth of the 12 rods.

Table IX. Control Rod Calibrations

Rod No.	Worth (Ih)
1	127
2	158
3	130
4	158
5	128
6	157
7	128
8	156
9	127
10	161
11	127
12	157
Total	1714 = 4.13% Δk

The total worth of the rods in several banked positions was measured using subcritical count techniques. Table X shows the total worth obtained from these measurements.

Table X. Total Worth of Control Rods

Banked Rod Position (in.)	Reactivity (Ih)	%Δk
14	0	0.0
11.5	-160	0.39
9	-475	1.15
7	-825	1.98
4	-1315	3.17
0	-1842	4.44
2 safety rods at 0 in.	-2365	5.70

d. Subassembly Replacements. The worth of an enriched uranium subassembly versus a natural uranium subassembly was measured at several core locations. Likewise, the worth of an enriched subassembly versus a depleted uranium subassembly was measured as a function of inner blanket location. All of the core measurements were subcritical, and the worths of inner blanket substitutions were determined by calibrated control rod changes. Table XI shows the results of these measurements.

Table XI. Worths of Subassemblies

Element Position	Worth (Ih)	%Δk
1 O 0	500	1.2
3 B 2	417	1.0
4 B 2	327	0.79
5 D 2	238	0.57
5 C 2	231	0.55
6 F 4	145	0.35
6 D 1	107	0.26
6 D 2	141	0.34
6 C 2	129	0.31

e. Isothermal Temperature Coefficient. The isothermal temperature coefficient is being determined by measuring the change in reactivity for a given change in reactor temperature. It is planned to measure the reactivity at 600, 550, 500, and 460°F. A preliminary measurement at approximately 500°F indicates the temperature coefficient over this range to be 1.05 Ih/°F.

f. Fuel Handling. In general, the performance of the fuel-handling equipment during the wet critical experiments has been satisfactory. However, some difficulties have been experienced with the rotating plug seals and the Fuel Unloading Machine.

With respect to the rotating plug seals, control of seal temperatures has become difficult, resulting in excessive time expenditure for temperature stabilization during the preparation for unrestricted fuel handling. It should be noted that the existing control systems will be replaced with improved equipment after the wet critical experiments have been completed. One seal trough thermocouple was found to be defective, and it was replaced. The seal heater circuits have been checked, and one has been found to be open.

With respect to the Fuel Unloading Machine, an accumulation of sodium and sodium oxide in the sodium vapor trap and associated piping and the transfer port caused excessive pressure drops in the recirculating argon system and excessive torque for rotation of the Fuel Unloading Machine port. The system was dismantled and cleaned.

2. Sodium Boiler Plant

At the beginning of the month, the steam generator and the associated secondary sodium piping systems were at ambient temperature. The temperature of the sodium in the dump tank was approximately 600°F and the plugging temperature had been reduced to less than 300°F by cold trap operation.

The temperature of the sodium in the storage tank was increased to 700°F. The plugging temperature remained below 300°F, indicating little or no further chemical reduction by the hot sodium of metal oxides presumably carried from the piping system into the tank during circulating and dumping of the sodium.

Following this high-temperature test, the sodium in the storage tank was cooled to 370°F for the next filling of the system.

A sample of magnetic material recovered from the sintered stainless steel filter which had been removed from the plugging indicator loop (see Progress Report for October 1963, ANL-6801, p. 16) was examined by chemical analysis and X-ray diffraction. Alpha-iron, iron oxides, and silica were found to be present. The silica was a minor constituent. The relative percentages of iron and iron oxides are not known, nor can it be said that the material recovered from the filter is necessarily representative of the bulk of the material in the system.

After cleaning, the filter was reinstalled in the plugging-indicator loop. However, during subsequent operation of the sodium system, continuing difficulties were encountered in the operation of the plugging valve and the flow-control valve. Apparently, a considerable amount of particulate material entered the plugging loop while the filter was removed. The behavior of these valves became so erratic that it was necessary to remove them. The plugging valve was replaced with a spare. Since no spare control valve was available, the plugging loop has been operated without a control valve.

During the week of November 11, the secondary sodium system was heated to approximately 360°F and filled. The system was then heated to near operating temperature for the first time. The steam drum pressure was 1260 psig and the sodium temperature was 570°F.

The plugging temperature rose rapidly during this heat-up. When it reached 500°F, the sodium was dumped. The system was then cooled to 350°F while the sodium in the storage tank was heated to 600°F.

The cold trap was operated with difficulty because of erratic and occasionally high differential pressure across the crystallizer tank. Nevertheless, it was possible to reduce the plugging temperature of the sodium in the tank below 300°F.

The system was filled again and heated to operating temperature. Once more, the plugging temperature increased rapidly, reaching 520°F about 48 hr after the sodium temperature reached 570°F. Since the temperatures of some drain lines were less than 520°F, the sodium was dumped to the storage tank to avoid plugging of lines with oxide.

It has been impossible to operate the cold trap at a rate greater than about 1 gpm for clean-up of the dumped sodium because of high pressure drop across the crystallizer tank.

It is believed that the cold trap contains approximately two-thirds of its theoretical capacity of sodium oxide, and an unknown quantity of iron and iron oxide. Therefore, it may have reached the end of its useful life. Work is underway to replace the cold trap with a spare, and also to install the cold trap previously used in the temporary primary purification system. The latter cold trap will be installed in the storage tank mixing line. Plans also call for installation of a magnetic separator in this same line to trap particles of magnetic iron oxide or reduced iron.

During the first system heat-up described above, attempted operation of the pump at 6000 gpm, the rated maximum capacity, was unsuccessful. The pump was shut down at 5000 gpm by the interlock which protects against loss of surge tank level. It was found that turbulence in the surge tank affects the behavior of the uppermost level indicator (with the associated surge tank level interlock for pump protection).

Inasmuch as the turbulence does not seem to affect the hydraulic behavior of the system, it is planned to move the interlock to a lower level indicator.

During the second heat-up of the secondary system, the interlock was bypassed and the pump was brought to full power at a system temperature of 460°F. The pump behaved well during this short test, delivering rated flow of 6000 gpm.

After the system temperature reached 570°F, a second test run was made and again the pump delivered full rated flow. It was planned to run the pump for 8 hr to determine thermal equilibrium conditions in the pump and its motor-generator set. However, approximately 45 min after the start of the test, the circuit breaker for the motor-generator tripped out. Since the motor was drawing only rated current, the protective relaying in the switchgear is suspect. Work is in progress to correct the situation.

During the month, 8 samples of argon blanket gas from the secondary storage tank were analyzed for apparent hydrogen concentration by gas chromatography. The concentrations ranged between 130 ppm (by volume) and 2500 ppm. The average of the 8 values is 750. No continuing trend toward increasing concentrations was observed over the month. It must be borne in mind that these samples may contain some helium which the gas chromatograph cannot distinguish from hydrogen (see Progress Report for October 1963, ANL-6801, p. 17).

Eight corresponding samples of blanket gas were taken from the surge tank. Analysis of one sample was invalid because of air contamination. The average of the remaining 7 reported values is 250 ppm (by volume) for a range between 140 and 640 ppm.

3. Power Plant

During November, activities in the Power Plant were directed largely toward support of operations in the Sodium Boiler Plant.

Early in the month the steam generator was in wet lay-up, completely filled with water chemically treated for corrosion inhibition. On November 11, circulating of water through the steam generator was started, preparatory to heat-up and filling of the secondary sodium system. During start-up of the Power Plant systems, the motor-driven feedwater pump was started to recirculate water through the pump and the deaerator (Heater No. 2), thereby accelerating heat-up. After a few minutes of operation, the oil temperature of the outboard thrust bearing was observed to be excessive. The pump was shut down and the cause of the high temperature of the bearing oil was investigated.

A manually operated valve in the pressure balance line between the pump and the deaerator was found to be closed. This condition had caused overloading of the thrust bearings, with resultant damage to both the inboard and outboard bearings. During the examination and repair of the damaged bearings, it was observed that axial movement of the pump rotor was less than the desirable "floating" travel, indicating possible internal damage to the pump. The pump manufacturer was contacted, and arrangements were made for a field representative to supervise the inspection and repair of the pump.

Disassembly and inspection of the pump disclosed minor internal damage. The balancing device was found to be slightly damaged; repair was accomplished in the field. The impeller and casing wear rings in one pump stage were found to be scored. A new casing wear ring was procured from the pump manufacturer. The impeller was repaired at the factory. Field repair was completed, and the pump was returned to operative condition before the end of the month.

The valve in the pressure balance line had been closed during a previous shutdown of the motor-driven feedwater pump and had been overlooked during preparations for the start-up in which damage was sustained as reported above. To prevent a recurrence of this incident, the valve has been locked in the open position.

The steam generator was heated from ambient temperature lay-up condition to 350°F by circulation and heating of boiler water. The evaporators and superheaters were maintained in flooded condition. Further heat-up from 350°F to 570°F during circulating of sodium in the secondary system was accomplished with the steam generator isolated by closing of the stop valves in the feedwater and blowdown lines. Steam-drum level was maintained by intermittent addition of feedwater to replace losses. A water level was established slightly above the centerline of the steam drum by draining boiler water. The superheaters and steam main were drained.

Hydrazine and morpholine treatment was maintained in the circulating boiler water. Prior to isolation of the steam generator and establishment of level in the steam drum, chemical feed rates were increased to provide ample treatment during static heat-up of the steam generator.

During the last week of the month, the steam generator was cooled to 350°F and then flooded. Boiler water was circulated by the start-up feedwater pump for completion of the cool-down to ambient. The steam generator was put into wet lay-up on November 27. The water is treated with morpholine, hydrazine, and sodium sulfite.

4. Fuel Cycle Facility

Despite low purification catalyst activity, it has been possible to maintain the purity of the Argon Cell atmosphere at a very high level for a period of two weeks, impurities being only about 5 ppm oxygen and 2 ppm water vapor. Inleakage effects were eliminated by holding the cell pressure slightly above atmospheric. This indicates the absence of major in-cell sources of oxygen and water vapor. A leak test at subatmospheric pressure indicated a rate of air admission of 0.005 scfm, in accord with earlier measurements. Instrumentation appears to be operable.

Gears to double the lifting speed (and reduce potential stress due to torque produced by the drive motor) will be installed on one of the Argon Cell crane trolleys for test purposes.

The Air Cell crane trolley has been repaired and replaced.

A study of the sheared, slotted, cylindrical spring pins (see Progress Reports for August and September 1963, ANL-6780, p. 17, and ANL-6784, p. 21) from Air Cell and Argon Cell operating manipulators has been made. These pins connect the driven half of a jaw clutch to the shaft of the bridge drive gear train on Air Cell and Argon Cell operating manipulators. The cause of the failure of these pins has been attributed to metal fatigue. The slotted cylindrical spring pins which are rated at 7700 lb in double shear have been temporarily replaced with solid alloy steel pins (Driv-Lok*) which are rated at 14,000 lb in double shear and are less subject to flexing under load than the slotted cylindrical spring pins.

Calculations of temperature profiles through the glass slabs in the 60-in.-thick shielding windows of the Argon Cell have been previously reported (see Progress Report for July 1963, ANL-6764, p. 19). Temperature gradients occur within a glass window as a result of the absorption of the gamma energy to which the window is exposed under plant operating conditions. Additional calculations have been made to show the effect on the temperature profile of the installed glass cover plates (see Progress Report for August 1963, ANL-6780, p. 16). The 1/4-in.-thick glass cover plates serve to protect the innermost (A) slabs of the shielding windows of the Argon Cell against mechanical stress which might lead to an internal electrical discharge in the slab (see Progress Reports for May and June 1963, ANL-6739, p. 45, and ANL-6749, p. 14). The following conditions during cell operations were assumed for the calculations: a gamma radiation intensity of 3.5×10^5 rad/hr, a cell ambient temperature of 100°F, an outer annulus temperature of 75°F, and a steady-state temperature of 147°F (owing to gamma absorption) for the steel shielding window shutters which were open for 8 hr and closed for 16 hr. The calculated temperature profiles show that with the steel shielding window shutter open, the maximum temperature at equilibrium (215°F) of the glass shielding window should occur at about 2 in. from the cell side (within the A slab) instead of the $4\frac{1}{2}$ in. (maximum temperature of 175°F) determined for shielding windows without glass cover plates.

Performance tests have been carried out on the battery that provides the power for the motor-blower assembly which recirculates the cooling gas in the Argonne-fabricated interbuilding coffin (see Progress Report for October 1963, ANL-6801, p. 24). The results of these tests show that, when the battery is fully charged, it can drive the motor-blower assembly to provide sufficient cooling capacity for the coffin for 8 hr.

The fuel-rod-breaking device for the decanner operates with a flying breaker bar. This has been found to produce a small chip of uranium-fissium alloy most of the time during the breaking of the rod

*A product of Driv-Lok, Sycamore, Illinois.

into short sections. It is diffucult to assure that the chips will be caught by the melt-refining-furnace charging tray and that they will flow out of the tray in the presence of clean sodium. It has not been possible thus far to break the rod without chip formation except by a true shearing operation.

There are preliminary indications that the high purity of the cell atmosphere may have introduced problems of sodium bonding of scrap and fuel to the decanner components. Investigations of the phenomenon have started.

The latest injection-cast melt produced 90 full-length castings from 91 molds charged. The gaging station was removed from the pin-processing machine and realigned. This corrected the feeding difficulties previously reported in this station. The data system for the pin-processing machine was recalibrated to indicate fuel-pin weight and length. The second fuel-rod welder was made operational and was successfully tested. The electrical insulation broke down in both welder feed-throughs during the tests. The feed-throughs have been repaired and reinstalled. Considerable electrical noise was induced into the bond-and-level inspection-machine transducer signals. This was corrected by isolation of the transducer signal leads in one of the spare feed-throughs.

Two melt-refining runs were made to blend fissium alloy for injection casting operations. Pouring yields of 96.2 and 96.9% were obtained. Two additional runs were made to compare pouring yields with broken rods, with and without about 3% of uranium chips produced in the fuel-breaking operation. The yields in these two runs did not appear to differ significantly, being in the range of 93-94%.

Welding of restrainers to empty fuel pin jackets was carried out in the Argon Cell. Both discharge welders were employed, and both appear to function satisfactorily when using all five "A" magazines available at the present time.

An injection casting run was made in which the casting pressure was reduced in an effort to reduce the number of hollow castings. No hollow castings were obtained, but the yield of pins greater than 15 in. long was only 50%.

Wiring and piping of the machine for the remote assembly of fuel elements is in progress at the Argonne, Illinois site. Magnesium oxide-insulated, copper-sheathed electrical cable is being used for radiation resistance. The bushings are being made from magnesium aluminum silicate (Lava). Dial indicators will be used to position the electrical gaging elements about the rotational center of the machine. Optical alignment methods will be used in the final inspection of the machine.

5. Process Development

a. Melt Refining of Uranium-Plutonium-Fissium Fuels. Preparations are being made to investigate the recovery of discharged uranium-plutonium-fissium fuels by an alternative melt-refining process performed beneath a molten salt layer. Advantages of this process found in small-scale experiments are higher yields and lowered operating temperatures. It is anticipated that the rare earth elements will be preferentially oxidized into the salt phase without significant oxidation and extraction of the plutonium. Preliminary experiments with uranium and various salt compositions, in order to determine a salt composition which would give minimum salt vaporization during a run and good salt-metal separation at the end of a run, were performed in a beryllia crucible contained in an argon-atmosphere induction-heated furnace. Melt refining consisted of holding the charge at 1150°C for one hour.

The most satisfactory salt flux thus far tested was 75 m/o barium chloride-25 m/o calcium chloride to which was added magnesium chloride in 10 percent excess of that which would have been required as a rare earth oxidant. Complete separation of this salt from a uranium ingot has been obtained in a two-pour operation in which the uranium was first solidified and the molten salt poured off at about 975°C. The uranium was subsequently poured at 1300°C. Under the standard melt-refining conditions, volatilization of the salt was negligible. Work with plutonium alloys has been started.

b. Skull Reclamation Process. Work was continued on the development of the skull reclamation process for recovery and purification of fissionable material in melt-refining crucible residues (skull material). In the latest run performed in the large-scale (2.5 kg of skull oxide) integrated equipment (see Progress Reports for April and July 1963, ANL-6717, p. 25; ANL-6764, p. 21), the process was modified to allow a single stationary transfer tube to be used. A stationary transfer line is very desirable for this equipment, since it is to be operated remotely. The modified process consists of (1) suspending oxidized skull material in a molten halide salt contained in a primary vessel and selectively extracting the relatively noble fission product elements into zinc, which is discarded, (2) reducing the uranium oxides and dissolving the uranium in a magnesium-zinc solution, (3) two precipitations of uranium out of magnesium-zinc solutions, first as U_2Zn_{23} (approximate composition), and then as uranium metal, with the supernatant magnesium-zinc solutions being discarded after each precipitation, (4) removal of the halide salt after the final magnesium-zinc supernatant is discarded instead of prior to the two precipitation steps, as in preceding runs, and (5) transfer of the uranium product (dissolved in a magnesium-zinc solution) to a second vessel and the retorting to yield a uranium metal product. In this run 89 percent of the zinc solution was transferred following the first step,

77 percent of the zinc-magnesium supernatant was transferred following the first precipitation, a total of 81 percent of the zinc-magnesium supernatant from the second precipitation was transferred, and only 60 percent of the halide flux was transferred prior to dissolution of the uranium in magnesium-zinc solution. An excessive amount of flux (15 percent of the original flux) was transferred to the retorting vessel with the dissolved uranium. It is expected that this problem can be readily solved, and further work with the modified equipment is planned.

In the skull reclamation process, a problem is created by the vaporization of salts (especially zinc chloride) used as process media and the deposition of these salt vapors throughout the furnace. For vapor control, a procedure was investigated in which all vapors from a mixture of calcium chloride, magnesium chloride, and zinc chloride heated to 800°C were passed through a bed of metal filings. Four experiments were performed, one each with uranium, calcium, magnesium, and iron beds. Zinc chloride fumes were completely removed in the experiments with uranium, calcium, and magnesium.

An eddy current induction probe for the remote determination of liquid metal levels is being tested in cadmium. (A similar probe is being evaluated in a cadmium still, as is described in this report in Sect. III.E.1.d.) The probe consists of primary and secondary nichrome coils on a ceramic core. High-frequency current is supplied to the primary. The output of the secondary is affected by the presence of external conductors such as a surrounding liquid metal phase. As presently constructed, the probe provides a linear change in output signal of about 1 mV/in. of cadmium. The effect of temperature on the output voltage of the secondary coil is 0.00047 mV/°C/in. of coil.

A silicon carbide crucible and a Type 410 stainless steel crucible which were plasma-sprayed with tungsten are being evaluated for the noble metal extraction and reduction steps of the EBR-II skull reclamation process. The crucibles, which are relatively large (of $10\frac{1}{2}$-in. O.D.), have each been subjected to a series of eight thermocycles in an argon atmosphere. The temperatures were alternated between room temperature and 900°C and between 300 and 900°C. At the conclusion of the temperature cycling, both coatings were intact and apparently undamaged. In additional tests, the crucibles are being contacted with molten zinc-magnesium-uranium and halide salt systems to determine their corrosion resistance to the skull reclamation process solvents.

Two thixotropically cast, high-density crucibles (manufactured by Coors Porcelain Co.) have been tested as follows:

(1) A $3\frac{5}{16}$-in.-O.D. by $3\frac{3}{4}$-in.-high beryllia crucible having a $\frac{5}{16}$-in. wall was contacted with zinc-magnesium at 700 to 800°C for 21 hr.

(2) An alumina crucible of the same dimensions was contacted first with a zinc-halide salt system at 800°C for 8 hr and then with a magnesium-halide salt system at 800°C for 4 hr. This test was repeated, using the same crucible.

Slight wetting of the beryllia crucible occurred near the air-liquid metal interface, and several long hairline cracks formed above the melt level. The alumina crucible was not undercut or wetted in the first test, but hairline cracks formed in the base and extended up the walls of the crucible. In the second test, slight penetration by the molten salt occurred. Crucibles of lower density, which are currently being prepared, are expected to be less subject to thermal shock than high-density crucibles.

c. Removal of Nitrogen from Argon. The removal of nitrogen from argon by gettering the nitrogen on hot (900°C) titanium sponge is under study. This study was undertaken because of the possible future need to remove nitrogen from the argon atmosphere of the Argon Cell in the EBR-II Fuel Cycle Facility. Construction of a 10-cfm pilot plant for obtaining information on component reliability is essentially complete.

d. Sodium Coolant Chemistry. The triton activation method was studied for the determination of 10 to 100 ppm oxygen in sodium metal. In this technique, the sodium is alloyed with a small amount of lithium, and then Li^6 (n, α)t and O^{16} (t,n)F^{18} reactions are induced by means of thermal neutrons. The fluorine-18 activity is then separated and counted. A standardization procedure for the irradiation has been established.

Work to develop a method for the analysis of carbon in sodium and to produce sodium of low carbon content has continued. A dry oxidation method, in which the carbon is oxidized to carbon dioxide with oxygen at 1100°C in a combustion train and the carbon dioxide produced is measured manometrically, is under development. A linear relationship has been demonstrated between the quantity of carbon found in sodium samples from a single source and the sample weights. Analytical results indicate that this sodium contained about 76 ppm of carbon. Sodium from the same source which had been gettered with zirconium for 10 hr at 550°C had a carbon content of 25 ppm.

6. Training

The wet critical operations (see Sect. D.1 above) afforded excellent opportunity for gaining experience in fuel handling, approaches to critical, measurement of reactor periods, determination of critical positions, banking

of control rods, small changes of power level, and shutdowns. Thirteen persons on the operating group are now qualified as Reactor Operators for wet critical operations in accordance with ANL procedures. Six additional reactor plant specialists who had met all the requirements for wet critical qualification, except actual nuclear operation, have acquired this operating experience.

Participation of reactor operator trainees during wet critical has been broadened to include several electrical, coolant, and steam specialists. A training log is maintained in the Control Room to record the individual Reactor Operator's experience.

A revised systems training format for new technicians has been prepared as a guide for supervisors in conducting training on a shift basis. One hundred four lesson plans outline the topics, scope, and experience required in preparation for qualification as reactor, electrical, coolant, steam, or power plant operators.

E. FARET

1. Design

The preliminary schedule as given in the Title I report (now being reviewed by the AEC) indicates start of excavation in July, 1964, and start of building substructures in March, 1965. Construction is scheduled for completion in February, 1967.

Bechtel has started the definitive design. An alternative building arrangement and a definitive design of the reactor vessel have been submitted for Laboratory review. Bechtel is presently reviewing the alternative design for cost, fabricability, and compatibility with existing design criteria.

Bechtel is also reviewing the engineering and construction schedule presented in the Title I report, which was prepared by the PERT critical path technique. Man-power leveling studies of the Bechtel design schedule are in progress.

The following key design problems are under consideration at the Laboratory:

(a) Review of the design concept of the argon process gas systems, especially in regard to purification, storage, and changing from gas to air in the cell, and vice versa. Consideration has been given to liquification, gas displacement, and vacuum systems.

(b) Review of viewing and lighting considerations associated with the cell. The use of remote viewing devices, such as television or periscopes, to supplement direct viewing through shielding windows is being studied. The type, size, and location of the windows are being defined.

(c) Study of cell and vault communications within these areas and between these areas and the rest of the plant. It is considered highly desirable that continuous communications be maintained between personnel within and without the cell. Communications are complicated by the use of breathing equipment for personnel who enter the cell when the atmosphere is argon.

A very simple working model of the cell has been completed and is in use. It will be used to assist Laboratory personnel to resolve design difficulties, such as viewing considerations, space allocation, and interrelationships between the movement of in-cell equipment.

2. Safety Analysis

The first draft of the Preliminary Safety Report, which is to be submitted to the Commission early in 1964, has been prepared.

3. In-core Instrumentation

a. In-vessel Connectors. An in-vessel connector test rig, consisting of a flanged stainless steel container, approximately 6 in. high and 3 in. in diameter, from which leads can be brought out through the flanges, was made leak tight. One sample high-temperature connector assembly was installed inside the test rig. In order to check out the initial operation of the rig and to minimize the possible problems, sodium was not added to the system. The system was, however, filled with argon and slowly heated. Measurements of the connector electrical properties were made at temperatures up to 500°C. At 400°C, the insulation resistance between any one terminal and the connector shell started to decrease very rapidly. This decrease continued after the system was brought up to 500°C. The test was discontinued when a stable insulation resistance had been reached. At this point, the insulation resistance had dropped from greater than 10^5 megohms to less than 100 ohms.

After cooling to room temperature, the rig was disassembled, and the connector and vessel inspected. A black powdery substance resembling powdered graphite was found on the outer portions of the connector body and inner surfaces of the test rig. The connector was disassembled and found to contain a considerable amount of this black carbon-like substance. The source of this substance was a coating on the metal interfacial seal gasket which evidently carbonized at roughly 400°C. This seal gasket had been supplied by the connector manufacturer for operation at temperatures above 650°C.

A second sample connector assembly, which is of all-welded construction and eliminates this gasket, is being made. Tests with this assembly will duplicate those with the first assembly.

b. Fuel Pin Thermocouples. When refractory oxide-insulated thermocouples are used to measure temperatures in the range from 1000 to 2800°C, a phenomenon known as the "distributed Seebeck battery"[2] must be considered (see Monthly Progress Report for June 1963, ANL-6749, p. 23). These distributed voltage sources coupled with a leaky cable usually introduce errors in the measurement.

These so-called "hot zone" errors can be determined when the thermocouple is treated as a dc transmission line having a generator (hot junction) with some internal resistance as a source, distributed series and shunting components of resistance along its length, distributed voltage sources (Seebeck batteries) along its length, and an infinite impedance load across the receiving end at null balance. Figure 4 shows an elementary equivalent circuit of this transmission line. The differential equations for this circuit can be shown to be

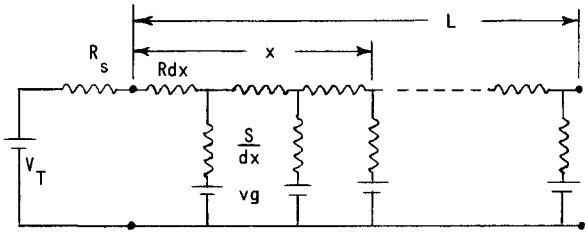

Figure 4. Thermocouple Equivalent Circuit

$$-\frac{dv}{dx} = R(x)i \tag{1}$$

and

$$-\frac{di}{dx} = \frac{v - vg(x)}{s(x)}. \tag{2}$$

Combination of Eqs. (1) and (2) yields

$$\frac{d^2v}{dx^2} - \frac{dR(x)}{dx}\frac{1}{R(x)}\frac{dv}{dx} - \frac{R(x)}{S(x)}v + \frac{vg(x)R(x)}{S(x)} = 0. \tag{3}$$

In these equations, v is the voltage at any point along the line, R(x) the wire resistance per unit length of line, S(x) the insulation resistance of unit length of line, and vg(x) the distributed voltage source along the line.

---

[2]High Temperature Thermometry Seminar, TID-7586, Part I, October 1 and 2, 1959, pp. 53-68, Oak Ridge National Laboratory.

Equation (3) can now be reduced to two first-order equations. Let

$$y_2 = \frac{dv}{dx} \tag{4}$$

and

$$y_1 = v. \tag{5}$$

From Eqs. (3), (4), and (5) we obtain

$$\frac{dy_1}{dx} = y_2 = f_1 \tag{6}$$

and

$$\frac{dy_2}{dx} = \frac{dR(x)}{dx}\frac{1}{R(x)}\, y_2 + \frac{R(x)}{S(x)}\,[y_1 - vg(x)] = f_2. \tag{7}$$

Equations (6) and (7) have been programmed for numerical solution on a digital computer by the Kutta-Merson Method.[3] The quantities R(x), S(x), and vg(x), determined by the temperature distribution along the line, and the physical properties and dimensions of the thermocouple materials, can be of any form. The only complication of this analysis is that it results in a two-point boundary value problem. The initial (hot junction) value of the voltage (v) is given and the final value of the slope dv/dx must be made zero. Because of the two-point boundary values, an iteration process must be used to find the final value of the voltage and, hence, the indicated temperature. This results in a computation time longer than normal.

Several types of thermocouples and temperature distributions are being studied. The results of these studies will be reported in subsequent monthly progress reports.

4. Reactor Vessel

The reference reactor vessel design[4] consists of a high-pressure cylinder, thermal baffles, an inner vessel, an outer vessel, and a support skirt. The inner vessel contains the bottom support structure for support of the high-pressure cylinder, the core support cylinder, and the core assemblies. Coolant is directed between the high-pressure cylinder and

---

[3] N. L. Fox, Numerical Solutions of Ordinary and Partial Differential Equations, Pergamon Press (1962) p. 24.

[4] FARET Title I Design Report, Bechtel Corporation.

the inner vessel into the coolant plenum chambers. The high-pressure coolant imposes an undesirable upward hydraulic force upon the core support cylinder. The design of the reference assembly provides several bolted parts which were rather inaccessible to hold down and to align the support cylinder. Replacement of the core support cylinder when changing from one reactor core type to another could be difficult under these conditions.

In an effort to simplify the design and to eliminate the bolts, an alternative reactor vessel arrangement was made as shown in Figure 5. The core support cylinder is self contained so that hydraulic forces are completely balanced internally, and bolting is not required. A double-walled reactor vessel contains the core support cylinders. There is only one flange connection to be made which is in the coolant inlet line and is readily accessible from the top of the vessel.

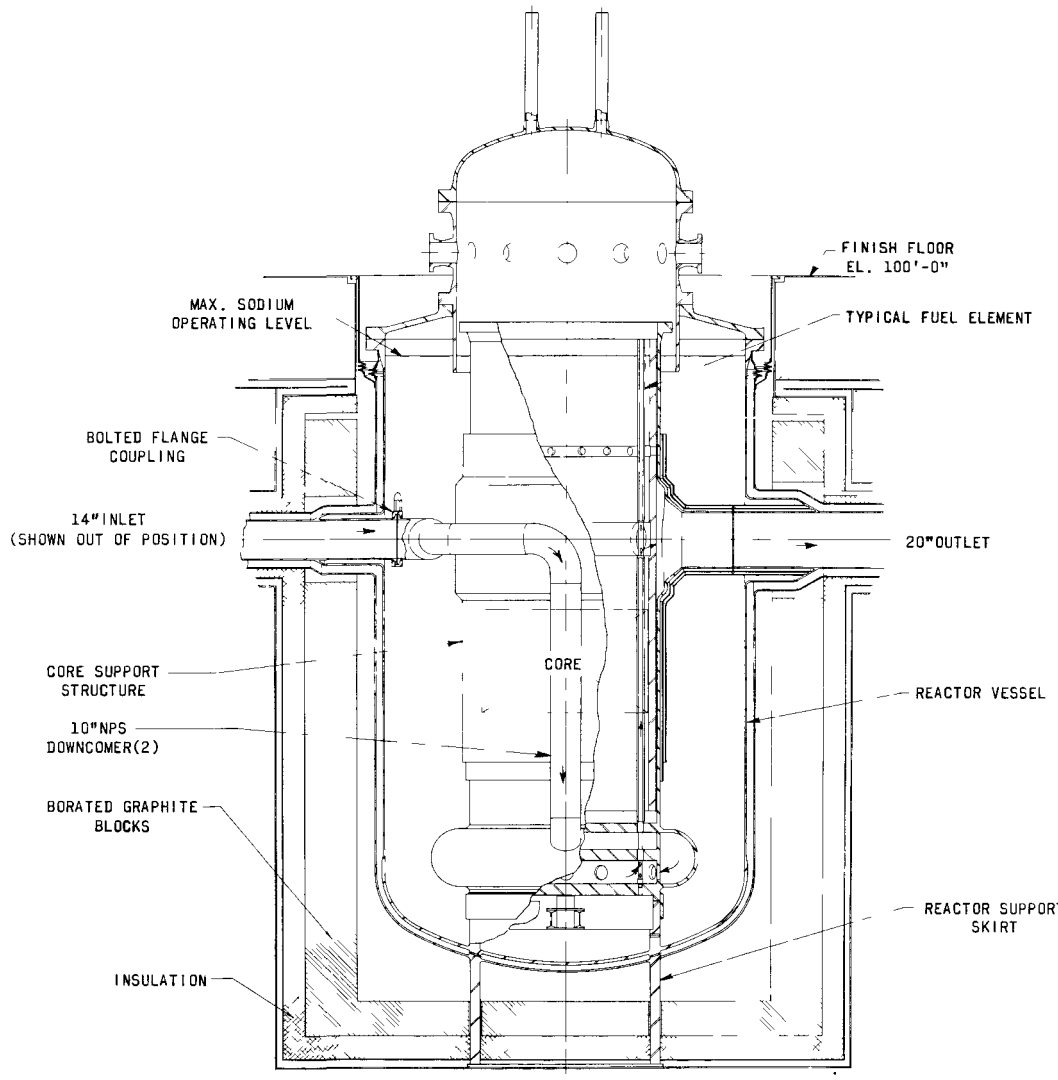

Figure 5. FARET Reactor Vessel Arrangement

Sodium enters the reactor vessel through a 14-in. pipe and is directed downward through two 10-in. pipes. These pipes or downcomers are connected to a toroidal-shaped chamber at the grid plate elevation from which sodium is distributed to a low- or high-pressure plenum of the core grid structure. Sodium flow through the low-pressure plenum, core, and upper outlet plenum is similar to that in previous systems. Flow is then directed through the core subassemblies or to the low-pressure plenum and reflector assemblies.

Although a reactor vessel of somewhat larger diameter (11 ft vs. 8 ft) is required, this increase in diameter may also be an advantage. For example, it may be adequate to compensate for sodium volume expansion and contraction due to temperature, thus suggesting the possible elimination of the surge tank. Finally, heaters may be accommodated more readily in the space between the inner and outer vessel. The effect of the change is being studied by Bechtel Corporation.

III. GENERAL REACTOR TECHNOLOGY

A. Applied Nuclear Physics

1. High-conversion Critical Experiment

The experimental program with the very heavily loaded water-moderated and reflected assemblies fueled with 3% enriched UO_2 is continuing. The assembly under investigation is uniformly loaded and has a 1.127-cm-pitch triangular grid. The assembly did not reach criticality because of limited fuel supply. The reactivity, however, can be raised by increasing the moderator content of the core. As mentioned in the Progress Report for October 1963, ANL-6801, p. 39, this can be done by removing one pin from each group of the 16, 12, 9, or 6 lattice cells throughout the core, thus increasing reactivity throughout the fuel zone. Another method is to increase the reactivity only in the periphery of the core, thus retaining the densely loaded central region for experimental measurements.

Data taken with a pattern of fifteen aluminum-clad fuel elements loaded per sixteen grid openings are given below. The atom ratio of hydrogen to U^{238} was 1.31. The fuel boundary was rectangular rather than cylindrical because of the limited size of the grid plate. The clean critical loading was 4937 ± 2.6 kg U^{235}. The rectangular dimensions required for criticality were 75.1 x 77.1 cm. Bucklings for the rectangular core were 10.7, 10.4, and 4.8 $cm^{-2} \times 10^4$ (axial direction) for a total of 25.9 $cm^{-2} \times 10^4$. Reflector savings were 20.8, 20.3, and 21.8 cm (axial direction). The estimated radial reflector saving (10.8 cm) for this atom ratio loaded in a cylindrical geometry coupled with the measured critical buckling values for the rectangular core leads to an estimated critical radius of 41.5 cm.

Micro-parameter measurements are now being done in a densely loaded central fuel zone of stainless steel clad fuel ($H:U^{238}$ atom ratio 0.99). The central zone of 10-cm radius is surrounded by an 18-cm-thick annular zone of aluminum-clad fuel. An 8-cm-thick peripheral region in which fuel density is halved (alternate rows left vacant) provides sufficient reactivity for criticality. Uncorrected capture cadmium ratio measurements for U^{238} were about 1.1 in the central zone.

Study indicates that application of a standard correction factor (F_{Cd}) for transmission of epicadmium- and subcadmium-cutoff energy neutrons by a cadmium cover may lead to significant error in cadmium ratio corrections for gold and indium activations. The correction for capture in U^{238} has not been obtained as yet. The cadmium ratio CdR(x,t), corrected for epicadmium absorption and subcadmium transmission by the cadmium, for a foil of thickness x covered by cadmium of thickness t, is given by

$$CdR(x,t) = \frac{Y(t)}{F(x,t)} CdR',$$

where CdR' is the observed, uncorrected cadmium ratio. CdR(x,t) is the cadmium ratio that would be observed for an ideal filter which changes sharply from black to transparent at the cutoff energy $E_{Cd}(t)$ as calculated for a 1/v foil.

Initial values obtained for the factor F(x,t) differ appreciably from the factor F_{Cd} sometimes used for this purpose. Further experimental work is needed, particularly in the case of gold, and also to verify the dependence of F_{Cd} on indium foil thickness. The possible effect of the misuse of F_{Cd} on the reported values of the resonance integrals for gold and indium should be investigated.

The evaluation of prescriptions to be applied to activation measurements for the densely loaded cores was undertaken because of doubt of their applicability in the hardened neutron-energy distributions encountered.

2. The Angular Distribution of Thermal Neutrons in JUGGERNAUT

Gold foils and gold spheres were activated in the South Test Cave of JUGGERNAUT in different geometries in order to measure the influence of the angular neutron distribution on self-shielding and to investigate the possibility of measuring the angular distribution of thermal neutrons by an activation experiment.

Gold foils, 1 cm^2 in area, and gold spheres, of 1-cm diameter, were activated in the center of cubic aluminum boxes inserted into the graphite of a thermal column. The boxes were lined on five sides with cadmium; the open side faced towards the reactor core. Cubes of the following dimensions and composition were used:

Cube No.	Size-Edge Length (cm)	Composition
1	20	interior void
2	20	interior graphite filled
3	10	interior graphite filled
4	5	interior graphite filled

Calculations of the angular distribution were based on data from the void box and by making a scaler flux plot with small gold foils in the graphite-filled boxes.

For the self-shielding measurements, foils of different thicknesses were activated, some facing the open side and others with their edge toward the open side. The measured self-shielding factor agreed with calculated values within the order of 1%. For the case of the 20-cm void box and the 5-cm graphite-filled box, an attempt was made to calculate the angular distribution from the self-shielding data. The results showed that a crude evaluation is possible, but that quantitative results depend upon extremely accurate self-shielding measurements.

The activation of the spheres was measured by a region-wise scanning technique which was done by placing a lead shield with a small collimating hole between the counter and the sample, and rotating the sphere into different positions. This method, too, yielded an essentially qualitative result for the angular distribution.

3. AFSR

Rossi-alpha was measured by means of two high-sensitivity He^3 neutron detectors. The results agreed, within experimental error, with earlier measurements made with conventional BF_3 proportional counters.

Since the core was recanned earlier this year, an increase in indicated air flow has been noted. This was due to a larger annulus surrounding the core pieces, which were slightly reduced in size after recanning. To verify that the indicated coolant flow represented an actual increase rather than a change in instrument calibration or in the bypass of air around the core, equilibrium core temperature measurements were made at 500 and 1000 W.

Power (W)	Flow (indicated, cfm)	Temperature (°C)				
		Air In	Air Out	Inner Blanket	Outer Blanket	Core
500	81	22.2	36.0	27.0	24.2	67
1000	80	24.5	51.6	34.0	29.0	110

Prior to recanning the core, it had not been possible to run at 1000 W for extended periods without exceeding the core temperature scram point of 125°C.

B. Theoretical Nuclear Physics

1. EBWR Core Designs

In previous reports (Monthly Progress Reports for September 1961, ANL-6433; and July 1962, ANL-6597), the feasibility of designing a

core for the EBWR to use depleted (0.2-0.4% enrichment) and slightly enriched (2.3-3% enriched) fuel elements was shown.

Using the Cycle 2 code, the reactivity versus burnup characteristics of a core having an EBWR lattice ($H_2O/UO_2 \simeq 2.82$) and a core having a more closely packed lattice (similar to that used in the Yankee reactor; $H_2O/UO_2 \simeq 1.29$) were calculated. In both core designs the ratio of depleted to enriched fuel elements was approximately 1 to 3. There were assumed to be no steam voids in the cores. Three-group cross sections, with Crowther-Weil prescription to allow for the high resonance capture in Pu^{240}, were used. The data obtained are shown in Tables XII and XIII.

Table XII. EBWR Lattice Core Design ($H_2O/UO_2 = 2.82$)

	Initially	1st Period	2nd Period	End Period
k_{eff}	1.0943	1.1023	1.0974	1.0943
Average burnup in enriched elements, Mwd/tonne	0	1,700	3,330	4,030

Table XIII Compact Core Lattice Design (H_2O/UO_2 1 29)

	Initially	Periods 1st	2nd	3rd	4th	5th	6th	7th	8th
k_{eff}	0 9968	1 0339	1 0427	1 0420	1 0365	1 0286	1 0191	1 0087	0 9979
Average Burnup Mwd/tonne									
in enriched elements	0	2 075	3 754	5 390	7 033	8 700	10 400	12 146	13 930
in depleted elements	0	678	1 500	2 437	3 476	4 603	5 819	7 125	8 512

Note Each period is roughly equivalent to 2500 Mwd/tonne (metric tonne) burnup in central enriched (2 7/1 element

According to these calculations the k_{eff} of the EBWR core lattice, when operating with no steam voids, will retain a k_{eff} value equal to or greater than its initial value for a burnup of about 4000 Mwd/tonne.

In the more closely packed pressurized reactor type of core, the average burnup of the enriched (2.7%) fuel elements is seen (Table XIII) to reach approximately 14,000 Mwd/tonne before k_{eff} reaches its initial value. During this period a burnup of ~8500 Mwd/tonne is obtained in the depleted elements.

It is apparent that the EBWR lattice core design will yield a burnup greater than 4000 Mwd/tonne, but the initial reactivity (k_{eff}) will be lower than shown in Table XII, if the reactor were operated with steam voids.

2. ZPR-VII Analysis

A report on the foil-activation program is being prepared. The report describes Fortran programs used to calculate quantities involved in foil activations.

Reactivities calculated for the Hi-C 1.24-cm square lattices using either aluminum or stainless steel clad and the Hi-C 1.27-cm triangular lattice with aluminum clad are found to be about 4 to 5% higher than the experimental data suggested. These calculations are based on THERMOS parameters for the thermal group and GAM-I parameters for the fast groups. The possible sources of the disagreement have been studied, and it is concluded that most of the discrepancy must lie in the GAM-I cross-section library.

3. Tungsten Cross Sections

To date $\sigma_f^{Np^{237}}/\sigma_f^{U^{235}}$ ratios, effective tungsten capture cross section, prompt-neutron lifetimes, and central boron worths have been computed for three initial ZPR-IX assemblies employing, in turn, tungsten cross-section sets Nos. 30, 35, 37, 40, and 43. The search for experimentally measurable parameters which would be sensitive to the differences in five tungsten cross-section sets was continued. A measurable (~5-15%) difference for some indices between the old set No. 30[5] and the other four more recent sets can be demonstrated. The calculations are now being extended to tungsten-reflected assemblies, and spectral indices are being calculated in the asymptotic reflector flux.

4. Worth of Boron and Boron Mixtures

A systematic effort is being conducted to evaluate theoretically the enhancement of boron worth by the proximity of other spectrum-lowering materials (carbon, aluminum, iron, and, especially, hydrogen). Results to date are quite promising in the sense that large increases in reactivity worth for boron mixtures with moderating materials have been predicted.

5. Prompt-neutron Lifetime and Effective Delayed-neutron Fraction

A comparison of $\beta_{eff}^{calc}/\ell_p^{calc}$ by diffusion theory and DSN transport methods of solutions have been carried out for ZPR-III fast assemblies No. 12 and No. 23 to determine whether or not the two methods of solution would give sufficiently different results so as to contribute in part to the presently generally observed discrepancy between calculated and experimental values. No substantial difference was found, however, by the two different methods of calculation.

---

[5] C. Cohn et al., Basic Material Resulting from ANL Rocket Study, ANL-6656 (May 1963).

C. Reactor Fuels Development

1. Corrosion Studies

a. Ferrous Alloys in Superheated Steam. Corrosion testing has indicated that Type 406 stainless steel has satisfactory resistance to superheated steam at 650°C and 42 kg/mm^2 (30 ppm O_2). It appears that the 4% aluminum contained in this alloy is largely responsible for its corrosion resistance, as shown by the poor resistance of similar alloys without aluminum. Type 406 stainless steel is not as satisfactory from the fabrication viewpoint, however, for it is very difficult to weld and grain growth is very pronounced during high-temperature brazing.

Amounts of aluminum, varying from 1 to 5 w/o, were added to Type 304 stainless steel in the small arc melting furnace and samples of Incoloy 800 containing aluminum additions were obtained from the International Nickel Company.

Data for one-week exposure to steam at 650°C and 42 kg/cm^2 (30 ppm O_2) are now available for the aluminum-modified 304. As little as 2 w/o of aluminum improved the film retention, but about 4 w/o was required to reduce the weight change to very small proportions.

b. Zirconium Alloys for Superheated Steam. Comparison is continuing of the corrosion behavior of as-cast samples of resistant zirconium alloys with that of hot-rolled samples of the same alloys. In 42.4-kg/cm^2 steam at 540 and 650°C all but one of the as-cast materials were more susceptible to blister attack than the hot-rolled specimens. The exception was Zr-Ni-Fe, which at 540°C developed few blisters and gained the least weight of all samples. After the first 100 days this material had gained 4.2 mg/cm^2, which is comparable with the 100-day gains of the most resistant zirconium alloys. The relatively poor performance of the other as-cast samples may be associated with blister formation. These results are consistent with the view that specimen microstructure as well as gross composition influences the corrosion behavior significantly. However, although efforts to optimize and stabilize microstructure may result in improved alloys for use at 540°C, present interest is in performance at higher temperatures, where alloy modification to control oxygen diffusion appears to be of primary importance.

Comparison of oxygen-absorption behavior with the corrosion weight gains of these materials in 650°C steam suggests that oxygen-diffusion rate and corrosion rate may not be directly related. Amount of oxygen absorbed did correlate with depth of surface hardening and perhaps with occurrence of surface blemishes.

Long-term exposure of Zr-4 a/o Ni and Zr-4 a/o Cu (as cast) to steam at 540°C and 42.4 kg/cm^2 has continued. After 300 days the Zr-Cu samples continue to gain weight at a decreasing and relatively low rate. Total weight gained averaged 5.6 mg/cm^2. Two of three Zr-Ni samples displayed an increased rate of weight gain after 200 days.

A sample of ANL-11 zirconium brazing alloy (Zr-8 w/o Ni-8 w/o Cr: M.P. 950°C) was tested in 42.4-kg/cm^2, deoxygenated steam at 540°C, a higher temperature than heretofore used with this material. The as-cast sample before test contained numerous cracks, which may not normally be present in thin brazed junctions. The material developed surface blisters and disintegrated between 50- and 100-day observations. Another sample was blistered but still intact after 49 days at 650°C.

c. Light Alloy Suitable for Use with Mercury at Elevated Temperatures. The study of inhibition of liquid-metal corrosion was continued with the titanium-mercury system. A thermal convection loop, made of 1.27-cm (0.5-in.) I.D. quartz tubing, was used. Pure nickel, in an amount calculated to give a concentration of about 700 ppm, was inserted in a cold branch of the loop. The location was chosen to limit the concentration of dissolved nickel to the solubility at the temperature of the coldest point in the system and to insure a continuous supply of inhibitor.

The loop was operated with a maximum temperature of 454°C in the hot leg and 320°C (coldest point) in the cold leg for a period of 90 days. The average flow rate was about 5.3 cm/sec (10.5 ft/min).

Visual examination of the exposed titanium samples indicated that no corrosion had occurred. Metallographic examination of a hot-leg sample showed the formation of a uniform protective layer, 8 μ thick. A weight gain of 1.86 mg/cm^2 was recorded. The small weight gain (0.42 mg/cm^2) and even surface on a cold-leg sample implied little or no corrosion at 353°C (average cold leg temperature). Spectrochemical analysis revealed that there was very little nickel deposition on the cold-leg sample. However, nickel concentration on the surface of the hot-leg sample was heavy. This observation will be checked by X-ray examination.

The phenomenon of thermal mass transfer to the hot leg is new and unexpected. Relatively little study has been made of the mechanisms of the inhibiting process. On the basis of the limited information accumulated, it may be that the thermal mass transfer observed here consisted of the dissolution of the soluble inhibitor transfer by diffusion and convection through the system to the surface of the solid, and subsequent interdiffusion. The temperatures at which the phenomenon occurs may be quite critical.

2. Ceramic Fuels

a. Irradiations of Uranium Sulfide. Six specimens of 6.42-mm (0.253-in.) diameter, pressed and sintered US pellets clad with 0.30-mm (0.012-in.) Nb-1 w/o Zr alloy, with a 0.05-mm (0.002-in.) helium annulus, have been examined after irradiation in the MTR reactor. Pellets of both 80 and 90% density were irradiated with half the specimens having an axial hole of 2.0-mm (0.080-in.) diameter through the entire length of the fuel section. Preliminary data were reported in the Progress Report for May 1963, ANL-6739, p. 32.

Isotopic burnup analyses indicated burnups ranged from 2.94 to 8.21 x 10^{20} fiss/cc (11,100 to 31,100 MWd/MT). Calculated cladding surface temperatures ranged from 400 to 790°C. The irradiation data based on the isotopic analyses are summarized in Table XIV.

Table XIV Irradiation of Uranium Sulfide

Spec No	Density, % Theory	Configuration	Burnup MWd/MT	Burnup Fiss/cc (x 10^{-20})	Clad Temp °C	Cladding Surface Heat Flux W/cm^2	Max Dia Increase cm	Vol Increase %	Gas Release % Theory
S-1	90	Solid	11,000	2 9	560	250	0 0025	0 17	0 05
S-3	90	Cored	14,000	3 8	400	170	0 0025	0 38	0 03
S-2	90	Solid	22 000	5 8	640	290	0 0025	0 26	0 11
S-4	90	Cored	31,000	8 2	790	360	0 0051	0 47	0 21
S-5	80	Solid	22 000	5 3	590	260	0 0204	1 0	20 0
S-6	80	Cored	23,000	5 4	540	230	0 0051	0 22	1 20

Fission-gas release from the 90%-density pellets was a maximum of 0.21%. One 80%-density specimen released 1.20% and the other 20.0%. The difference in gas release is attributed to basically closed porosity in the denser pellets and essentially interconnecting open porosity in the less dense pellets. The 20% release from the one specimen, S-5, is attributed to an as yet unexplainable temperature transient. This same specimen had a small circumferential bulge at the top of the fuel section.

Metallographic examination of the 90%-density specimens showed no significant changes from unirradiated samples. A Widmanstätten structure of very fine needles was present in both. These needles tended to disappear toward the center of specimen S-4, which achieved the highest temperature. The needles were only faintly present in a few grains of the finer-grained 80%-density pellets which were originally sintered at 1700°C. The 90%-density pellets were liquid-phase sintered at 1925°C; the 80%-density pellets were not. The composition of the needles is presently unknown.

Sections through the overheated specimen, S-5, showed excessive amounts of a second phase that has been identified as UOS. The center

of the specimen contained an irregularly shaped core of a coarser porosity that was devoid of the UOS phase. The core was about 35% of the pellet diameter. The equiaxed grain size in this region was 0.08 mm, which may be compared with 0.05 mm for the rest of the specimen and the unirradiated material.

A longitudinal section through the bulge in this specimen showed that the bulge was immediately adjacent to a central cavity. The cavity was surrounded by an area of high porosity, some columnar grains of US, and massive areas of UOS. The porous area is believed to connect with the porous center core found in lower regions of the fuel. A tantalum spring at the top of the fuel, used to keep the pellets from separating, was half gone; the remaining half showed evidence of reaction with the sulfide. Particles believed to be melted tantalum were also found in areas of UOS at the base of the cavity and the periphery of the pellet.

A temperature transient is the suggested cause of the center core and the melting at the top. The lack of significant grain growth or sintering in areas adjacent to the core is the primary evidence for this belief. The immediate cause of melting and formation of the cavity at the top would be the inability of the helium gas space to dissipate the heat generated during the transient. The top fuel pellet was in immediate contact with the gas space. Since considerable fission gas was released, the transient did not occur early in the irradiation period. Specimen S-6, irradiated under almost identical conditions of heat generation and cladding temperature in the same reactor position, showed none of the adverse conditions found in S-5. The only difference was the 2.0-mm-diameter axial hole in S-6.

b. Preparation of Uranium Monosulfide. Preparation of uranium monosulfide on a 100- to 300-g scale is continuing. Hydrided-dehydrided uranium powder is treated with hydrogen sulfide, and the sulfide product is homogenized by heating to about 1900°C. Examination of the results of nine runs performed at sulfur-to-uranium atom ratios of 0.95 to 1.04 shows that the lattice parameter at sulfur-to-uranium ratios of 0.99 to 1.02 remained constant at the theoretical value of 5.489 to 5.490 Å. At ratios above and below these values, the lattice parameters decreased.

c. Preparation of Uranium Monocarbide. An additional 400-g batch of uranium carbide has been prepared by adding activated charcoal to uranium dissolved in zinc-14 to 18 w/o magnesium at 800°C and stirring at 350 to 400 rpm for 8 hr. In this run, the oxygen content of the uranium monocarbide was reduced to 0.20 w/o. The main effort is being directed toward the preparation of products having carbon contents near the theoretical content of 4.80 w/o, low oxygen contents, and small particle size, so that grinding prior to pressing and sintering will not be necessary.

d. Preparation of Plutonium Carbides. Studies are being performed to investigate various chemical procedures for the preparation of plutonium carbide. A laboratory-scale experiment was conducted in which Mg_2C_3 was reacted with $PuCl_3$ for 0.5 hr in a 35 m/o lithium chloride-65 m/o magnesium chloride salt system at 650 to 675°C. The volatile components (mainly lithium chloride and magnesium chloride) were then distilled at 870°C and 0.03 torr in a period of about one hour. X-ray diffraction analysis of the residue showed the product to be primarily Pu_2C_3, with minor amounts of PuOCl present as an impurity.

3. Particulate Metal Fuel Elements

a. Vibratory Compaction. Since the last reporting period, 20 experiments on the compaction of binary shot mixtures were carried out with both spherical and irregularly shaped shot. Graphical representation of the results showed that the packing of spheres within a matrix of spheres follows a mathematical relationship which is very similar to the packing of spheres within a tube. Although the results must be analyzed further, it appears that the packing fraction may be expressed in terms of the following general equation:

$$Pf = A - Be^{-k(D/d_1)} - Ce^{-\ell(d_1/d_2)} - Ee^{-m(d_2/d_3)}$$

where Pf is the total packing fraction, A the limiting packed density, B, C, and E constants dependent upon particle shape, k, ℓ, and m constants whose dependency is yet unknown, D the diameter of the container, d_1 the diameter of the coarse fraction, d_2 the diameter of the medium fraction, and d_3 the diameter of the fine fraction. Work is continuing on the study of ternary sphere mixtures and binary systems of irregular shaped particles.

Preliminary sodium-bonding experiments have been run on the sodium-bonding of metal shot. EBR-II-sized Vycor molds were loaded with shot. Metallic sodium was placed on top of the shot. The tubes were then evacuated to less than 20 μ. The sodium was melted and then pressurized with one atmosphere of helium. Twenty-three-cm-long, 0.368-cm-diameter columns of 125-μ grit bonded full length. Seventy-five-micron grit columns of similar size bonded for a length of 20 cm. Grit less than 44μ also bonded over approximately 20 cm of the 23-cm column. Additional work is in progress to determine the correct parameters for bonding the finer grit. The effectiveness of the bond was determined by sectioning and metallographic study of the bonded specimens.

4. The Thorium-Uranium-Plutonium System

Thorium-plutonium alloys with uranium additions are potential high-temperature nuclear fuels for fast breeder reactors. The alpha-phase

boundaries shown in Figure 6 are the result of metallographic observations and lattice-parameter measurements, and indicate the limits below which no liquid phase occurs at 700 and 900°C. Some of these thorium-base alloys may actually be $\alpha + \beta$ or β-phase alloys at the high temperature. Room-temperature metallography offers no indication in that respect, since the beta phase is not retained at room temperature upon quenching. On the other hand, lattice-parameter measurements indicate that the beta phase perhaps does occur in this temperature range. However, more work is required to corroborate the evidence.

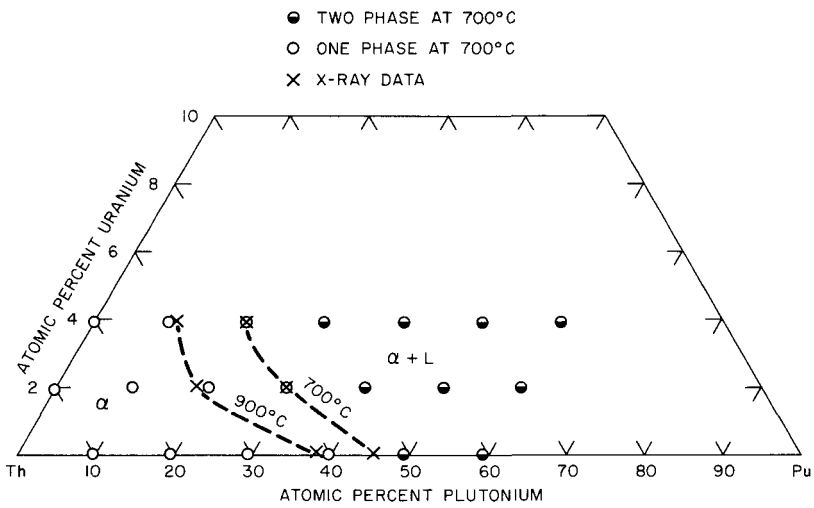

Figure 6. Thorium-Uranium-Plutonium Alloys. $\alpha \rightleftharpoons \alpha + L$ Solidus

Investigations of the effect of heat treatment on the lattice spacing of high-purity crystal-bar thorium reveal an increase in the lattice spacing with time and temperature of heat treatment (see Table XV). The observed changes are not likely to be caused by contamination during heat treatment, since the heat treatment was made with bulk material that was protected by a tantalum-foil wrapper and sealed under vacuum in Vycor

Table XV. Lattice Spacings of Crystal-bar Thorium (B794) before and after Heat Treatment

Lattice Parameter a_0, Å at 25°C	Heat Treatment Temp (°C)	Time (hrs)	Cooling
5.0840	As Received		
5.0842	700	2	Furnace Cooled
5.0848	700	2	Oil Quenched
5.0855	900	2	Furnace Cooled
5.0857	900	2	Oil Quenched

tubes. Needle specimens were prepared by grinding after the heat treatment. The specimens were stress relieved under the same protective conditions. The lowest value of a_0, 5.0840 Å, is in excellent agreement with, but slightly lower than, the best literature values. The slightly lower value of this investigation reflects the higher purity of our material. Its theoretical density is 11.728 g/cm^3.

The crystal-bar thorium which we have used in these experiments was analyzed by our Chemistry Division and the analytical results are shown in Table XVI.

Table XVI. Analysis of Crystal-bar Thorium (B794) (Data in ppm)

Chemical Analysis		Spectrochemical Analysis**	
H:	2	Al:	7
C:	7	B:	High*
N:	5	Fe:	30
O:	45	Hf:	Low*
Si:	10	Ti:	0.5
		Y:	2
		Zr:	10

*Data for B and Hf are suspect and are being checked by other methods.

**All other elements below limits of spectrochemical detection.

Limits of Spectrochemical Detection:

Ag:	1	Co:	1	Li:	0.005	Sb:	20
Al:	1	Cr:	0.5	Mg:	1	Sn:	2
B:	1	Cu:	5	Mn:	0.1	Sr:	0.005
Ba:	0.2	Ga:	0.5	Mo:	0.5	Ti:	0.2
Be:	0.002	Hf:	0.5	Na:	1	V:	0.5
Bi:	2	Fe:	5	Ni:	1	Y:	0.02
Ca:	2	K:	2	Pb:	1	Zn:	2
Cd:	2	La:	0.2	Rb:	0.5	Zr:	0.2

An alloy with the composition 60 w/o Th-20 w/o U-20 w/o Pu, as injection cast and as heat treated, is presently being encapsulated for irradiation.

Other potential fuel alloys of thorium with 10 and 20 w/o Pu with 4 w/o U added appear to be attractive because of their nuclear and also

their metallurgical properties. These alloys have a face-centered cubic matrix. We are testing them for compatibility with Type 304 stainless steel at a temperature of 650°C. Densities of homogenized castings of these and other Th-U-Pu alloys are given in Figures 7 and 8 and in Table XVII. The measurements were made by the hydrostatic weighing method with an accuracy of better than ± 0.005 g/cm^3. The scattering of the data with 40% plutonium and more is due to ingot segregation.

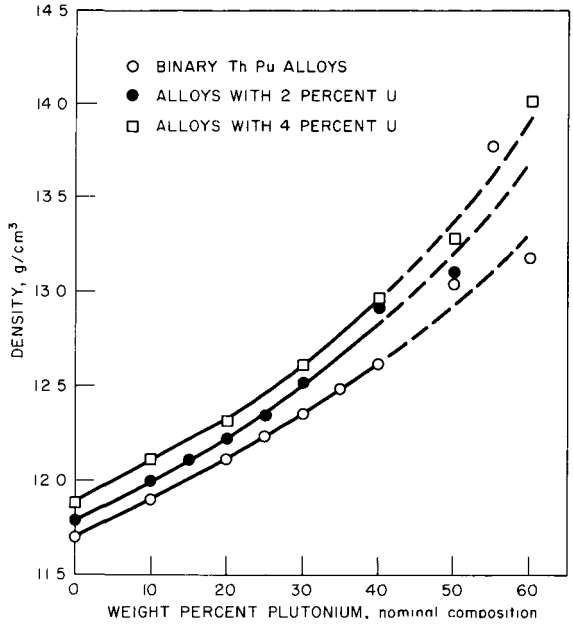

Figure 7. Density of High-purity Th-Pu and Th-U-Pu Alloys Annealed 3 Weeks at 700°C and Water Quenched

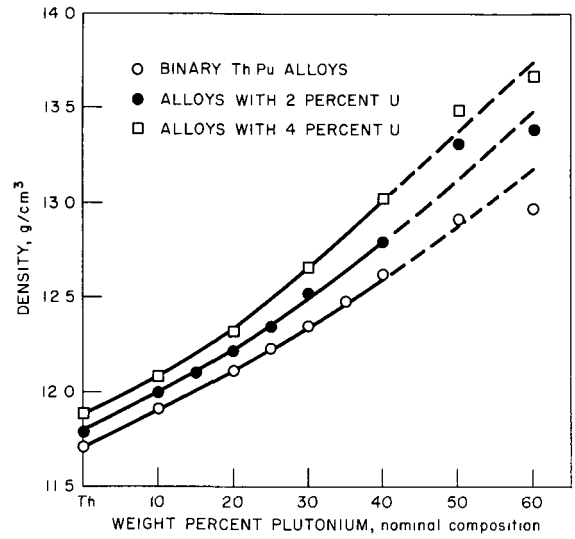

Figure 8. Density of High-purity Th-Pu and Th-U-Pu Alloys Annealed 3 Days at 900°C and Water Quenched

The factors influencing the precision of density measurements in gloveboxes were investigated. An important factor was found to be differences between the temperature of the glovebox atmosphere and of the liquid surrounding the specimen during weighing. A revised formula taking into account these temperature differences was derived.[6]

---

[6] B. Blumenthal, Density Measurements in Gloveboxes - with Density Data on Monobromobenzene, Cast Thorium, Thorium-Uranium and Thorium-Plutonium Alloys, ANL-6671.

Table XVII. Densities of Binary and Ternary High-purity Thorium-Uranium-Plutonium Alloys

Nominal Composition (w/o)			Density (g/cm^3)	
Th	U	Pu	Annealed 3 Weeks at 700°C and Water Quenched	Annealed 3 Days at 900°C and Water Quenched
100	-	-	11.699	11.712
90	-	10	11.902	11.908
80	-	20	12.108	12.115
75	-	25	12.228	12.227
70	-	30	12.347	12.352
65	-	35	12.478	12.477
60	-	40	12.613	12.618
50	-	50	13.04	12.92
45	-	55	13.77	12.99
40	-	60	13.16	12.97
98	2	-	11.788	11.793
88	2	10	12.002	11.991
83	2	15	12.114	12.103
78	2	20	12.224	12.216
73	2	25	12.345	12.345
68	2	30	12.515	12.517
58	2	40	12.81	12.79
48	2	50	13.10	13.31
38	2	60	14.05	13.39
96	4	-	11.881	11.886
86	4	10	12.111	12.081
76	4	20	12.340	12.315
66	4	30	12.614	12.656
56	4	40	12.97	13.03
46	4	50	13.28	13.49
36	4	60	14.01	13.67

5. Zero-power Reactor Fuel Materials

The cast specimens of 67 a/o U-27 a/o Pu and various additional alloying elements, described in the Progress Report for September 1963, ANL-6784, p. 13, have been subjected to a one-month corrosion test in air. The specimens were placed in an air-atmosphere glovebox through which room air at the rate of 15 cfm was drawn. The temperature was nearly constant at 24°C. The relative humidity varied from a low of 25% to a high of 56%. Specimens of U, U-30 a/o Pu and U-20 w/o Pu-10 w/o Fz were also run for comparison. Table XVIII summarizes the results. Figure 9 shows the condition after 21 days.

Table XVIII. Effect of Room Air on Uranium and Uranium-Plutonium-base Alloys

Alloy*	Original Weight (gm)	Weight after 1 Month (gm)	Remarks
U-27 Pu-6 Al	6.87	7.78	Began gaining weight on 2nd day. Completely disintegrated by 6th day.**
U-27 Pu-6 C	3.23	3.62	No gain in weight first 5 days. Gained 0.03 gm 6th day. Completely disintegrated by 6th day.**
U-30 Pu	6.85	7.50	Began gaining weight on 2nd day. Completely disintegrated by 6th day.**
U-27 Pu-6 Cu	4.45	4.79	Did not begin gaining weight until 7th day. Although showed some signs of swelling and initial disintegration on 6th day. Completely disintegrated on 21st day.**
U-27 Pu-6 Fe	2.95	2.95	No change in weight. Slightly tarnished.
U-27 Pu-6 Zr	3.75	3.75	No change in weight. Slightly tarnished.
U-27 Pu-6 Mo	3.49	3.49	No change in weight. Slightly tarnished.
U-20 Pu-10 Fz†	0.10	0.10	No change in weight. Slightly tarnished.
Uranium	3.20	3.20	No change in weight. Slightly tarnished.

* Compositions given in weight percent.

** Still gaining weight after 30 days.

† U-20 Pu-10 Fz in w/o.

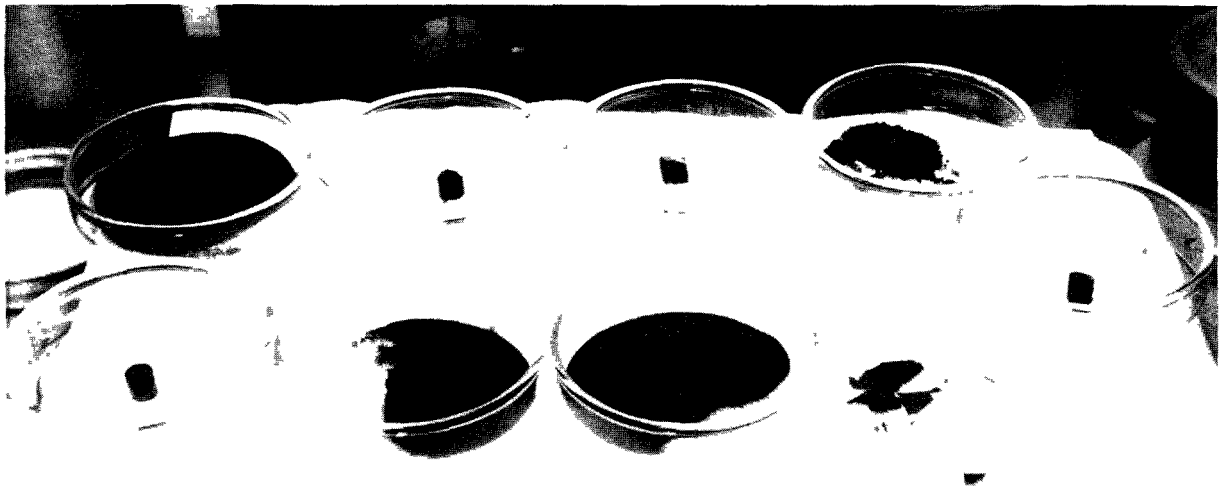

Top Row: U-27 a/o Pu-6 a/o Al, U-27 a/o Pu-6 a/o Fe, U-27 a/o Pu-6 a/o Zr, U-27 a/o Pu-6 a/o Cu
Extreme Right: Uranium
Bottom Row: U-27 a/o Pu-6 a/o Mo, U-27 a/o Pu-6 a/o C, U-30 a/o Pu, U-20 w/o Pu-10 w/o Fz.

Figure 9. Pyrophoricity Samples after 21 Days in Air

6. Nondestructive Testing

a. Neutron Imaging. Further studies on the light emission from several neutron scintillators have indicated that the light output from the scintillators appears to be saturated at the neutron intensities normally used with the Juggernaut neutron radiographic facility. As the neutron intensity is decreased by reducing reactor power, however, a reasonable change in light intensity is found. This indicates that it may be possible to obtain improved contrast sensitivity by means of scintillator-film techniques for neutron radiography if the neutron intensity is properly adjusted. Film studies to verify this are now in progress.

The neutron facility has been used to inspect a number of heavy-metal objects including two tungsten castings, 4 cm and 6.3 cm in diameter. The neutron inspection of 280 cm of 2.5-cm-diameter steel-molybdenum-tungsten extrusions was also accomplished.

Other neutron inspection work completed during this report period includes the neutron inspection of two irradiated, reactor fuel capsules, and several test radiographs of Borax superheater fuel assemblies.

b. Ultrasonic Imaging. Resolution studies on aluminum test plates containing flat-bottomed holes have yielded resolution results similar to those previously reported (see Progress Report for October 1963, ANL-6801, p. 48) for test objects containing holes completely through the plate. Similar results have also been found for nonbond test objects in which flat cover plates have been bonded over the flat-bottomed hole samples.

These studies have been made with the test object oriented perpendicularly to the ultrasonic beam direction. Since recent data have indicated that much improved visual detection of objects can be obtained if the sample is oriented at angles on the order of 15 to 20° from this perpendicular, further resolution studies at various angular positions are now in progress.

Initial evaluation studies of the sealed ultrasonic camera tubes have been completed. These studies indicate that at least two of these quartz target tubes show good response to ultrasound. The studies also tended to confirm previously reported data[7] that quartz showed improved sensitivity and decreased resolution properties as compared to barium titanate as a target material.

---

[7] J. E. Jacobs, H. Berger, and W. J. Collis, An Investigation of the Limitations to the Maximum Attainable Sensitivity in Acoustical Image Converters, IEEE Trans. on Ultrasonic Engineering, UE-10, 83-88 (Sept 1963).

c. Correlation of Heat-Transfer Properties and Bond Quality. Two modifications were made in the flash-tube apparatus for determining thermal diffusivity. The discharge capacitor was changed from 50 μf to 250 μf. This increased the energy output of the tube from 400 to 2000 Joules, and the back surface temperature of a typical specimen from about 1.5°C to about 3°C. The flash-tube trigger pulse was increased from 10,000 to 40,000 V; this insures the flashing of the tube with every trigger pulse.

The physical set-up was made mechanically rigid, so that neither the settings of the optical system for a condition of uniform illumination of the specimen nor the quantity of heat reaching the specimen will vary in the course of a series of measurements.

The condition of uniform illumination was difficult to achieve with an optical system. In the process of establishing this condition, it was found that a piece of overexposed X-ray film placed in specimen holder showed any variations in light intensity occurring on the front surface of the specimen. This method is now used as a fast check for the illumination condition.

The reproducibility of the system was checked in two ways. In the first, the thermocouple contact position on the back surface of the specimen was kept the same, and between measurements the specimen was removed from the holder and then reinserted. Each of ten measurements made this way showed a temperature rise of 3.0°C. The half-rise time varied by 3%. For copper this is a time difference of less than 0.1 ms, a difference easily attributable to the actual reading of time from the Polaroid print.

In the second way, the copper specimen remained in the holder and the thermocouple position was changed so as to scan the whole back surface of the specimen. In the 24 measurements made, the temperature rise was 3.0°C, and the half time varied by 3%. This is not true when any of the outer edges of the specimen are scanned, as heat is lost much more rapidly here with the result that the maximum temperature is less.

d. Application of Infrared Radiation to Nondestructive Testing. A focusing device has been installed in the optical head of the mechanically scanned infrared-imaging system. A small lamp illuminates the detector and the detector image is projected on the object plane. The mirror system can then be adjusted to form a sharp image. The area on the object covered by the detector image exactly determines the area being inspected. A variable diaphragm has been placed in front of the detector to improve resolution for higher-temperature objects.

D. Heat Engineering Research

1. Two-phase Nozzle Flow

The existing literature on two-phase nozzle flow has been critically examined. Considerably more information is available for two-component rather than single-component two-phase flow in converging-diverging nozzles in the low-quality region. Although efficiencies and relative velocities between the phases in two-component systems have been reported, no direct information can be found for one-component systems.

Two quantities which are important in evaluating the efficiency of nozzle performance are: (a) the slip velocity of the mixture, and (b) the extent to which the flowing fluid attains equilibrium between the vapor and the liquid phase.

Only one source of data was found for one-component, two-phase low-quality flow through nozzles.[8] Two nozzles were employed in the above tests. Nozzle I had a throat diameter of 0.438 in. and an exit-to-throat area ratio of 5.6:1. Nozzle II had a throat diameter of 0.250 in. and area ratio of 25:1. The thrust of the leaving fluid stream was measured in addition to the usual measurements of flow rate and pressure profile throughout the nozzles. Flow rate ratios varied from 0 to 0.2 lb. steam per lb mixture, and initial pressures varied up to 1000 psia. No attempt was made to measure or calculate slip ratio or the efficiency of the nozzle.

These data were therefore examined in detail for information on slip ratio, nonequilibrium effects, and efficiencies of the nozzles. The efficiency as used here is defined as the ratio of the actual kinetic energy of a unit mass of the leaving liquid phase to the kinetic energy of a unit mass of fluid expanding ideally, assuming no slip and equilibrium between the phases.

A set of equations was developed for the computer such that exit slip ratios of the nozzles could be calculated from the experimental information provided thermodynamic equilibrium prevailed.

The following results were obtained: The slip ratio, k, varied from 1 to 5 in Nozzle I, and from 0.6 to 2.0 for Nozzle II. Slip ratios less than 1.0 were obtained for Nozzle II when the flow was overexpanded in the diverging section. The slip ratio seemed to be independent of total pressure drop, ΔP, across the nozzle for a given flow rate, and very definitely increased with increasing flow rate. Since calculated slip ratios are found to be independent of ΔP, it is believed that the higher slip ratios obtained

---

[8] E. S. Starkman, Expansion of A Very Low Quality, Two-phase Fluid Through A Convergent-Divergent Nozzle, ASME Paper 63-AHGT-4.

for Nozzle I were mainly due to nonequilibrium effects. The departure from equilibrium would be expected to be much greater in Nozzle I than II, since Nozzle I had a much shorter diverging section, and hence a shorter flow time for a given flow rate. It was shown that a reduction in quality below the value obtained from assuming thermodynamic equilibrium resulted in lower calculated slip ratios with all other quantities remaining the same. It can, therefore, be concluded that the slip ratio calculated represented an upper bond.

The following ranges of efficiencies were calculated based on the obtained slip ratio: Nozzle I, 10 to 80 percent; Nozzle II, 35 to 95 percent. These results indicate that a properly designed nozzle can give an efficiency of as high as 90 percent.

E. Chemical Separations

1. Chemistry of Liquid Metals

a. Solubility of Plutonium in Cadmium. The solubility of plutonium in liquid cadmium over the temperature range from 335 to 632°C may be represented by two empirical equations:

$$(335 \text{ to } 399°C): \quad \log(\text{a/o Pu}) = 6.223 - 4282\ T^{-1};$$

$$(399 \text{ to } 632°C): \quad \log(\text{a/o Pu}) = 5.148 - 5277\ T^{-1} + 1.156 \times 10^{6} T^{-2}.$$

b. The Yttrium-Zinc System. X-ray data for the yttrium-zinc system confirm the existence of the phase YZn_{12}, previously suggested by the results of effusion studies (see Progress Reports for January and March 1963, ANL-6683, p. 39, and ANL-6705, p. 47). Additional effusion data on the yttrium-zinc system were used to evaluate the equilibrium zinc vapor pressures of intermediate phases of this system at various temperatures. The values obtained agreed well with results[9] determined by means of the dew-point method.

c. Praseodymium-Cadmium Galvanic Cell Studies. The thermodynamic functions of the praseodymium-cadmium system are being evaluated by means of a galvanic cell. A new cell of the form $Pr/PrCl_3$, LiCl-KCl (eutectic)/Pr-Cd (two-phase alloy) has been assembled, and the emf of the cell has been measured as a function of temperature. The free energy of formation of $PrCd_{11}$ may be represented by the equation

$$\Delta Gf° = -61{,}004 + 20.92\ T - 1.77 \times 10^{-2} T^{2}$$

over the temperature range from 360 to 540°C.

---

[9] P. Chiotti, J. T. Mason, and K. J. Grill, Trans. Met. Soc. AIME, 227, 910 (1963).

d. Liquid Metal Distillation. In fuel-recovery processes with liquid metals and fluxes, a method is required for the remote determination of liquid levels and interfaces between liquid metals and fluxes. An eddy current induction probe (described in this report in Sect. II.D.5.b) for continuously measuring liquid levels has been evaluated in the large unit for distillation of cadmium. The use of the probe led to reliable values of the cadmium level in the still pot during charging and distillation. A probe of this type gives promise of being an effective and accurate device for monitoring the metal liquid level in a remotely operated distillation unit.

To obtain information on temperature distribution in the cadmium-distillation unit, vertical temperature profiles have been obtained in the still pot during distillations. The temperature from the top to the bottom of the liquid region was constant, as was the temperature in the vapor phase, although about 25°C lower than the temperature in the liquid region. Comparison of measured liquid cadmium temperatures with a calculated boiling point curve (assuming 22 mm Hg pressure in the vapor phase) indicated that boiling could have occurred only within the top inch of liquid cadmium in the still pot.

With power inputs of 20 to 40 kW, the apparent distillation rates in the cadmium distillation unit (fitted with a de-entrainment device) were 39 to 92 kg/hr and the apparent power efficiency ranged from 32 to 57 percent. The effectiveness of the de-entrainment device will be determined when analytical results are obtained for five runs in which lead was used as a tracer.

Study of the nonturbulent vaporization of mercury from a 1-in.-diameter, 12-in.-deep liquid pool was continued. In three runs, in which the rate of vaporization was about 115,000 Btu/(hr)(sq ft), surface superheating of mercury through the vaporizing surface averaged 28°C above the vapor space saturation temperature. A large superheat is believed to be an important part of the mechanism for nonturbulent vaporization at high rates. The driving force for the vaporization process depends upon the superheat attainable before vapor bubble nucleation starts.

e. Plutonium Recovery Process. Development work was continued on the use of ternary cadmium-zinc-magnesium alloy as a process medium for the recovery of plutonium-bearing fuels. Such a medium may allow the use of lower process temperatures and stainless steel equipment.

The solubility of uranium in three additional alloys (Cd-20 a/o Zn-20 a/o Mg, Cd-20 a/o Mg-13 a/o Zn, and Cd-20 a/o Zn-13 a/o Mg) has been measured at temperatures of about 375°C to 650°C or 700°C. For these alloys and alloy compositions studied previously (see Progress Report for October 1963, ANL-6801, p. 57), uranium solubility increased with increasing zinc concentration and decreased with increasing magnesium concentration as shown below:

Zn(a/o)	Mg(a/o)	Cd(a/o)	Uranium Solubility at 600°C (w/o)
-	-	100	2.1
13	13	74	3
13	20	67	2.2
20	10	70	4.4[a]
20	13	67	3.5
20	20	60	2.7
100	-	-	0.2

[a]Measured at 650°C.

Uranium-bearing solid phases in equilibrium with the solutions under various conditions have been identified by means of metallographic examination as alpha-uranium, the delta uranium-zinc intermetallic compound ($\sim U_2Zn_{17}$), and UCd_{11}.

f. Distribution of Californium between Magnesium Chloride and Zinc-Magnesium. The distribution of californium-252 between liquid zinc-magnesium alloy and magnesium chloride is being determined as part of a study of transplutonium element separations in liquid metal-salt systems. Preliminary results indicate that californium strongly favors the flux phase at magnesium concentrations below 20 w/o, but that it shows an increasing tendency to distribute to the metal phase as magnesium concentrations were increased from 20 to 84 w/o. This behavior has not been observed with any of the other elements investigated thus far (see Progress Report for April 1962, ANL-6565, p. 27). Preliminary results of experiments carried out at 750, 800, and 850°C indicate that the behavior of californium was also different from that of the other elements inasmuch as californium was found to distribute increasingly to the metal phase (zinc-14% magnesium alloy or magnesium-34% zinc alloy) with decreasing temperature.

2. Fluidization and Volatility Separations Processes

a. Recovery of Uranium from Low-enrichment Ceramic Fuels.

(i) Laboratory-scale Fluid-bed Fluorinations. Laboratory support work has been directed toward the establishment of optimum conditions for the fluid-bed fluorination of mixtures of U_3O_8 and plutonium dioxide (see Progress Report for September 1963, ANL-6784, p. 50). Two additional fluorination runs have been carried out with U_3O_8-PuO_2 mixtures containing added fission product oxides. The concentration of plutonium in the U_3O_8-PuO_2 mixtures was about 0.4 w/o, and the concentration of 11 fission product oxides (La_2O_3, CeO_2, Pr_6O_{11}, Nd_2O_3, Sm_2O_3, Eu_2O_3, Gd_2O_3, Y_2O_3, BaO, ZrO_2, and MoO_3) was about 0.86 w/o. In these runs, alumina was added to the mixture prior to being fed to the fluid-bed

reactor. The fluorination reaction sequence consisted of two steps. The first step was a fluorination-feeding period during which the feed material was continuously transported into a $1\frac{1}{2}$-in.-diameter fluidized bed of alumina and simultaneously reacted with 20 v/o fluorine in nitrogen. The second fluorination step was carried out with 100% fluorine which was recycled through the fluid bed.

In the first run, the fluorination-feeding period ($2\frac{1}{2}$ hr) was performed at 450°C and was followed by three successive recycle-fluorination periods of 5 hr at 450°C, 5 hr at 500°C, and 10 hr at 550°C. After this series of recycle fluorinations, the residual uranium and plutonium contents of the alumina bed were 0.015 w/o and 0.007 w/o, respectively.

In the second run, the fluorination of six batches of feed material was carried out with one bed of alumina (initially unused). The following operating conditions were used. The fluorination-feeding period (1 hr) was conducted at 500°C for six successive batch additions of feed material (U_3O_8, PuO_2, fission product oxides, and alumina). After the sixth batch addition of the feed material, the alumina bed was then fluorinated for two recycle-fluorination periods of 10 hr each at 500°C and 550°C, respectively. Following each reaction period, the alumina was removed from the reactor, and a sample taken for uranium and plutonium analyses. The alumina was then replaced in the reactor for re-use in a subsequent step in the run.

Recycled alumina was also used to prepare the second through sixth batches of feed material for the fluorination-feeding periods. Fresh alumina was only added to the first batch of feed material. The results of this run showed that, during the fluorination-feeding periods, the residual plutonium concentration of the alumina bed increased rather regularly for the first four batch additions of feed material, from 0.10 w/o to 0.42 w/o, and then decreased to 0.23 w/o after the sixth batch addition of feed material. After the recycle-fluorination periods at 500°C and 550°C, the residual plutonium concentrations of the alumina bed were 0.19 w/o and 0.18 w/o, respectively. The final residual plutonium concentration of 0.18 w/o corresponds to a retention on the alumina of 13% of the total plutonium (6.98 g) fed to the fluid-bed reactor. The final residual uranium concentration of the alumina was 0.01 w/o, which corresponds to about 0.003% of the total uranium (about 1510 g) feed.

These results tend to verify previous small-scale, boat-type experiments (see Progress Report for October 1962, ANL-6635, p. 44) in which relatively high retention of plutonium by alumina was observed when the initial fluorination temperature was 500°C. However, much lower plutonium retentions were obtained in the first run and in previous boat experiments[10] in which the initial fluorinations were carried out at a lower

[10] ANL-6648, Chemical Engineering Division Summary Report, October, November, December, 1962, p. 130.

temperature (450°C). The residual plutonium concentration of the alumina in these experiments varied from 0.003 to 0.009 w/o. Because of the much lower plutonium retentions obtained at 450°C, the effect of the lower temperature will be investigated in the current series of fluid-bed experiments.

(ii) Engineering-scale Studies of Two-zone Oxidation-Fluorination Processing Scheme for Clad Uranium Dioxide. The alumina bed from a previous two zone oxidation-fluorination run (see Progress Report for October 1963, ANL-6801, p. 60) was subjected to a cleanup fluorination step for further removal of uranium. Prior to the fluorination step, the UO_2 stainless steel cladding was removed from the reactor. During the cleanup step, the fluorine was introduced at the bottom of the fluid-bed reactor. The fluorination step was carried out at 500°C for a period of 4.5 hr of total off-gas recycle with fluorine added to a maximum concentration of 68 percent. This cleanup step resulted in reducing the residual uranium concentration in the alumina to 0.72 w/o, which is greater by a factor of 10 than the uranium retained by the alumina in other runs. Further study is planned to determine if the retention of uranium in the alumina is increased by re-using alumina and by using alumina of smaller particle size (hence, increased available alumina surface area). The alumina in this run had been used in a previous run (see Progress Report for July 1963, ANL-6764, p. 53), and consisted mainly of small particles, 86% of the particles being in the size range of -120 +200 mesh.

b. Recovery of Uranium from Highly Enriched Uranium-Alloy Fuels by Chlorination and Fluorination Steps

(i) Bench-scale Studies. Studies of the feasibility of using a fluid-bed chlorination-fluorination scheme for the recovery of enriched uranium from uranium-alloy fuels were continued. Presently, tests are being carried out with uranium-aluminum and uranium-Zircaloy fuels. The work is being conducted in a $1\frac{1}{2}$-in.-diameter fluid-bed reactor with the alloy subassembly being submerged in an inert bed.

Recently, another run using a multiplate uranium-aluminum fuel subassembly has been carried out (see Progress Report for September 1963, ANL-6784, p. 52). The objectives of this run were to determine (a) the effect on the retention of uranium by alumina of the addition of simulated fission products to the fluid bed, (b) the effect of interruptions of feed gas streams (which would allow the fluid bed to become static) and of elevated bed temperatures (to 600°C) on the fluid-bed behavior of the alumina bed, and (c) the disposition of the silicon from the silicon-aluminum alloy brazing rod used in the fabrication of the test fuel subassemblies charged in this test.

In this run, the charge consisted of four uranium-aluminum subassemblies (total weight 176.7 g; ~4 w/o normal uranium), each subassembly being 5 in. long. In the fabrication of these subassemblies, the

uranium-aluminum plates were brazed with a 12 w/o silicon-aluminum rod (Castolin*) instead of being welded with type aluminum-1100 rod (greater than 99 w/o aluminum). In addition to the subassemblies, 13.7 g (4.1 w/o of the reactor bed) of 11 simulated fission products were also charged to the fluid-bed reactor. The eleven fission products were strontium, yttrium, niobium, molybdenum, ruthenium, rhodium, antimony, tellurium, cesium, barium, and cerium. Sintered alumina grain (Tabular T-61, Aluminum Company of America) was used as the inert material in both the fluid-bed reactor (320 g; -40 +120 mesh) and packed-bed filter (640 g; -14 +20 mesh).

The following reaction sequence was employed in the run: hydrochlorination, hydrofluorination, and fluorination. The hydrochlorination step was conducted at fluid-bed and filter-bed temperatures of 280°C (average) and about 180°C, respectively, for 6.4 hr. The hydrofluorination step (50 v/o hydrogen fluoride in nitrogen) was conducted at an average fluid-bed temperature of 350°C for 1 hr. This was then followed by two fluorination periods, one of 4 hr at a fluid-bed temperature of 250°C, and the other of 2 hr at a fluid-bed temperature of 500°C. In both fluorination periods, the fluorine concentration was increased stepwise from 5 to 90 v/o (remainder nitrogen). The filter bed was maintained at the same temperature as the fluid bed during the hydrofluorination and fluorination reaction steps.

The planned interruptions were carried out during and after each reaction step of the processing cycle. During these interruptions, the feed gas stream was stopped, thus causing the alumina in the reactor to become static, and the temperature of the reactor was cycled for varying periods between room temperature and 600°C. During the reaction steps, the interruptions consisted of stopping the gas flow and rapidly cooling the reactor from its operating temperature to room temperature, maintaining the reactor at room temperature for 2 hr and then reheating the reactor to operating temperature. After each reaction step, the interruption involved stopping the gas flow and heating the reactor assembly (fluid-bed reactor and packed-bed filter) to 600°C, maintaining the assembly at this temperature for 2 hr, and then cooling it from 600°C to its operating temperatures.

The retention of uranium by the sintered alumina in the fluid-bed reactor was apparently unaffected by the presence of relatively high residual concentrations (1.3 w/o of the fluid bed) of simulated fission products. The final uranium concentration in the bed was 0.01 w/o (0.5 w/o of the uranium initially charged). This concentration is the same as the low level achieved previously in a run made without added simulated fission products (see Progress Report for September 1963, ANL-6748, p. 52). The rate of uranium loss (0.7 mg/hr) through the packed-bed filter during hydrochlorination was the lowest achieved in the current series of

*A product of Eutectic Welding Alloys Corporation.

runs in which the feed charges were either uranium-aluminum alloy chips or uranium-aluminum subassemblies The total uranium loss for the hydrochlorination period amounted to 0 1% of the uranium initially charged. This low uranium loss is believed to be due to the increased height (12 in.) of the filter bed. In previous runs (see Progress Reports for June 1963 and September 1963; ANL-6749, p 46, and ANL-6784, p. 52), filter bed heights of 6 and 8 in. were used. A comparison of the filtration efficiency* data for all runs with uranium-aluminum alloy chips or uranium-aluminum subassemblies indicates that the optimum filter bed height is about 8 to 10 in.

The sintered alumina in the fluid-bed reactor did not cake and was readily refluidized despite the planned interruptions. The presence of the simulated fission products also did not affect the behavior of the alumina bed. Preliminary results indicate that about 90% of the simulated fission products that were added to the fluid-bed reactor were retained by the alumina beds in the reactor and filter. The distribution of the individual fission product elements appears to be in conformity with the distributions estimated from the volatilities of their higher-valent chlorides and fluorides.

The silicon from the brazing alloy was retained primarily, and rather unexpectedly, by the alumina in the fluid-bed reactor and the packed-bed filter. The silicon concentration in the alumina was 0.6 w/o

(ii) Pilot Plant Demonstration Runs. Two additional shakedown runs have been completed in the pilot plant installed to demonstrate the fluid-bed fluoride volatility process for recovering uranium from highly enriched uranium-alloy fuels. In each run, a subassembly composed only of Zircaloy or of aluminum was charged to the fluid-bed reactor. In these runs, only the hydrochlorination and hydrofluorination reaction steps were carried out. In future experiments with subassemblies containing uranium, the fluorination reaction step will also be carried out. During the hydrochlorination step, the fluid-bed pyrohydrolysis reactor was operated simultaneously for converting the volatile zirconium tetrachloride** or aluminum trichloride (each of which represents a waste stream) to their respective solid oxides.

The operating conditions for the two runs are shown in Table XIX. In both runs, operational performance was considered highly satisfactory. Fluid-bed reactor temperatures were satisfactorily controlled by means of the reactor coolant system which regulated the reactor

*Filtration efficiency is defined as the ratio of the quantity of uranium which is passed through the filter to the quantity of uranium which is loaded on the filter.

**Tin chloride (from the Zircaloy) was probably also present.

wall temperature to within about five degrees of the set point. The fuel charges were completely reacted in the hydrochlorination times indicated. The shorter hydrochlorination reaction time in the run with the Zircaloy-only subassembly (5 hr) than that in the run with the aluminum-only subassembly (11.7 hr) resulted from higher total gas flows, a sustained period of higher hydrogen chloride concentration, and higher bed temperature. Maximum temperatures of 710°C and 335°C were observed in the channels between the plates of the Zircaloy-only and aluminum-only fuel subassemblies, respectively. Since the temperatures sustained in the aluminum run were so well controlled and were well below the melting point of aluminum (660°C), a significant increase in reaction rate can probably be achieved without exceeding practical operating temperature limits. The present Zircaloy reaction rate is considered satisfactory.

Table XIX. Operating Conditions for Fluid-bed Hydrochlorination and Hydrofluorination of Zircaloy-only and Aluminum-only Fuel Subassemblies

Fuel Subassembly Charge:	Zircaloy only; 13.6 kg; 3 ft long Aluminum only; ~13.7 kg; ~4 ft long
Equipment (all nickel):	6-in.-diameter fluid-bed reactor 9.5-in.-diameter packed-bed filter 6-in.-diameter pyrohydrolysis reactor
Inert Bed Material:	Alumina. In the run with the Zircaloy-only subassembly, sand was used in the pyrohydrolysis reactor.
Reaction Steps:	Hydrochlorination and hydrofluorination (fluorination step omitted because no uranium was present in either subassembly used)

Run Charge (subassembly)	Zircaloy Only	Aluminum Only
Hydrochlorination Period		
HCl, v/o in nitrogen	46 to 62	55
Reaction time, hr	5	11.7
Temperature, °C		
Reactor Bed, avg	400 to 500	300
Packed-bed filter	390	275
Pyrohydrolyser	360	300
Avg Utilization Efficiency, %	43	55
Hydrofluorination Period		
HF, v/o	20	20
Reaction time, hr	1	1.8
Temperature, °C		
Reactor bed	375	330
Packed-bed filter	390	275

Preliminary results obtained during the pyrohydrolysis of the volatile chlorides from the hydrochlorination of the subassemblies indicate that some particle growth did occur in the run with the aluminum-only fuel subassembly. The particle growth results from the deposition of solids on the starting bed material. However, the major fraction of the aluminum oxide was found to be in the form of fines smaller than 100 mesh. The pyrohydrolysis reactor operated satisfactorily, and bed temperatures were uniform. In the two runs, the pressure drop across the sintered metal filters remained at a low level.

3. General Chemistry and Chemical Engineering

a Head-end Treatments for Refractory Fuels. A process for dissolving uranium monocarbide fuels in molten chloride salts has been further investigated. The dissolution procedure used previously (see Progress Report for October 1963, ANL-6801, p 63), which produced free carbon and (probably) a U(IV) species, was modified and was as follows: Hydrogen chloride was bubbled through molten NaCl-KCl containing a UC pellet at 750°C for 2 hr to break up the pellet and dissolve the uranium, the temperature was raised to 900°C, and carbon dioxide was passed through the melt for $1\frac{1}{2}$ hr, the temperature was decreased to 750°C, and the melt was sparged with hydrogen chloride for another 45 min. After the melt was filtered, only a small amount of carbon residue remained on the walls of the tube, carbon having been removed by the reaction of carbon with carbon dioxide to form carbon monoxide. The product was a green salt solution containing about 10 w/o uranium, as calculated from the weights of the starting materials.

4. Calorimetry

A series of seven combustions of niobium diboride in fluorine has been completed. Calculations are in progress.

Satisfactory techniques for the calorimetric combustion of thorium in fluorine have been developed.

F. Plutonium Recycle Program

1. Plutonium Recycle Fuel

The following fuel loading is being fabricated for the Plutonium Recycle experimental core:

(a) A central zone of mixed plutonium oxide-uranium oxide fuel elements, to be supplied by General Electric, Hanford. This zone contains 36 elements fueled with 1.5 w/o plutonium oxide and 98.5 w/o depleted uranium oxide.

(b) An intermediate shim zone fueled with enriched uranium, to be fabricated by United Nuclear Corporation. This zone contains 60 elements fueled with UO_2 enriched to 6 w/o U^{235}.

(c) A blanket zone of natural uranium, to be fabricated by United Nuclear Corporation. This zone contains 58 elements fueled with natural UO_2.

The PuO_2-UO_2 fuel for the central zone is being prepared at Hanford by the Dynapak process described in the September Progress Report, ANL-6784, p. 56. Approximately $\frac{1}{3}$ of the fuel material required for this central zone has been prepared. Facilities for processing the fuel loading at Hanford are completed.

United Nuclear Corporation's Chemical Division has converted all the natural UO_3 to UO_2 for the blanket fuel rods. This natural UO_2 has been tested for composition and pellet density, and is reported to be satisfactory. Facilities and equipment are being prepared for fuel loading, welding, handling, and inspection at United Nuclear Corporation's Fuels Division. Schedules are being established for delivery of subcontracted hardware components, including Zircaloy-2 fuel cans, fuel jacket tubing, end plug stock, and fuel element grids and end fittings.

2. Physics Program

The IBM 704 code 1188/RE has been used to calculate β_{eff} and ℓ for the hot voided system at zero burnup, the cold system at zero burnup, the cold system at 0.006 burnup, and the cold plutonium critical configuration at zero burnup. The respective values for β_{eff} are: 0.00494, 0.00534, 0.00660, and 0.00307. The corresponding values for the prompt-neutron lifetime, ℓ, are: 30.9, 25.5, 26.1, and 41.7 μsec. The values for the hot system differ from those reported in Progress Report for October 1963, ANL-6801, p. 67, owing to a computational error.

As expected, the plutonium critical configuration has the smallest value for β_{eff}. The shift in β_{eff} to the larger value at 0.006 burnup is due to the power shifting out from the plutonium zone into the uranium zones of the system.

The above values have been used with the RP 130 code to calculate period versus reactivity, and with the RP-129 "J" code to evaluate integrated energy versus reactivity input.

The cold system at zero burnup releases an integrated power of 1000 MW-sec for a step insertion of k_{eff} = 1.016. At 0.006 burnup, 1000 MW-sec is generated for k_{eff} = 1.0147. For the plutonium critical configuration, 320 MW-sec are released with a k_{eff} = 1.014. These

energy releases correspond roughly to melting of the oxide fuel at the hottest point in the core. The asymptotic periods corresponding to the above reactivities are 2.4, 3.2, and 3.8 msec, respectively, for the cold system at zero burnup, at 0.006 burnup, and for the plutonium critical configuration. These periods are all long compared with the upper limit of 1.2 msec for the time delay calculated[11] for the heat transfer from the plutonium to the uranium in the mixed oxide fuel.

Calculations by means of the ARGUS code are being used to examine thermal stresses in the Zircaloy cladding as well as cladding temperatures for the various severe reactivity insertions considered above. Preliminary results are in agreement with SPERT experiments[12] and calculations[13] which indicate there is only a small energy transfer to the clad during the small time intervals involved in the excursions being considered.

Rod worths and reactivity coefficients are being calculated by the PDQ-3 and RE-122 codes. At zero burnup, the nine rods are worth about 17% and the central rod about 4%. The reactivity swing from hot operating to the hot no-void condition is about 8%. This corresponds to about 11% after allowing 3% for xenon and other uncertainties. For the cold system but with the water assumed to be at the hot no-void density condition, k_{eff} is about 1.12, whereas for the cold system k_{eff} is about 1.15.

For the plutonium critical configuration at zero burnup, the nine rods are worth about 16% and the central rod is worth about 10%.

---

[11] R. E. Peterson, Time Delay in the Doppler Effect Resulting from Inhomogeneities in Mixed PuO_2-UO_2 Fuels, HW-78711.

[12] T. M. Quigley and A. H. Spans, Calculation and Measurement of the Transient Temperature in a Low Enrichment UO_2 Fuel Rod during Large Power Excursions, IDO-16773 (May 18, 1962).

[13] T. R. Bump and R. W. Seidensticker, Analysis of Temperatures and Expansions Resulting from Exponential Power Changes in a Reactor, Nuclear Sci. and Eng. 4, 44 (1958).

IV. ADVANCED SYSTEMS RESEARCH AND DEVELOPMENT

A. Argonne Advanced Research Reactor (AARR)

1. Core Physics

As a possible means for alleviating serious flux distortion during the time of maximum insertion of control rods and as a possible means of extending core lifetime, a brief study of spectral shift control as applied to AARR was made. The study showed that spectral shift control can furnish about 13% δk swing; however, flux and power peaking problems are aggravated by this type of control, and it was judged to have no advantage for AARR.

All calculations for the AARR are now being conducted for a 40-40 core (fuel plate and coolant channel thicknesses each equal to 0.040 in.). The fluxes and adjoint fluxes have been determined at 21°C and 100°C with new cross-section sets, divided into eighteen energy groups. The cross sections of plutonium-239 and zirconium have been added to the sets. Thermal upscattering is included for three groups and downscattering for five. The thermal flux in the core decreases roughly by 10% from the values obtained using the old 16-group cross-section set with no upscattering. The prompt-neutron lifetime, β_{eff}, and the power distribution are being determined with the new fluxes and adjoint fluxes as input.

2. Critical Experiment

The contract for fuel required in the critical experiment is still under negotiation. Delivery depends upon the date of execution of the contract. At present it appears that delivery may not commence before April or May, and fuel loading into the critical facility is not likely to occur before June or July, 1964.

Unexpected difficulty was encountered during checkout of nuclear instrumentation for the critical experiment. Incompatibility was found between various circuits. The trouble was traced to oscillation and noise originating in three separate chasses. Although inconsequential at their origins, the disturbances were amplified and propagated by associated equipment, and the low-flux circuitry was entirely disabled when tested under operating conditions. The individual chasses perform satisfactorily when isolated.

The equipment had been purchased on an individual lowest-bid basis, and several brands and bidders had become involved. The resulting assortment is difficult to service and operate. In addition to the cost of investigating and modifying this equipment, there is a possibility that some components may have to be replaced before satisfactory operation is obtainable.

This was the first console obtained by ANL through competitive bidding on individual components. Others have been purchased subsequently on a package basis. Either approach results eventually in a considerable diversity of equipment. Other National Laboratories have claimed that substantial improvement was gained by specifying standardized components rather than by submitting reactor consoles for competitive bids.

3. Reactor Control

Alterations permitting the use of the 100-MW transient study analog program for transient studies at 240 MW (conforming to a 40-40 core) have been completed. Provisions for studying the effects of variations in system pressure and coolant flow velocity were added to the program.

A literature survey and a study of Fortran programming methods have been carried out preliminary to the preparation of a comprehensive digital code for use in future AARR transient studies.

4. Beam Tubes for the Experimental Facility

Prior to building a two-dimensional analog simulation model for determination of temperature distribution in the AARR beam tube thimbles, the Franklin Institute has completed a preliminary series of thermal gradient and stress studies in order to set the bounds on the allowable wall thicknesses. These studies basically consisted of the following: (1) for a fixed inside diameter of the beam tube, the outside diameter was continuously varied, and the temperature difference between inside and outside wall and average temperature difference were determined as functions of heat generation rates; (2) for a fixed inside diameter of the beam tube, the outside diameter was continuously varied and the total heat flux integrated to determine the total amount of heat to be removed from the beam tube wall; (3) from the information obtained by the first group of curves, combined stresses were obtained as a function of the outside diameter for fixed inside diameter, various outside pressures, and 100-MW and 240-MW power levels.

These calculations provide the information required for the preliminary selection of the wall thickness for each of the beam tubes. In addition, the coolant flow requirements can be established for any wall thickness selected. The calculations performed by Franklin Institute appear to be consistent with preliminary calculations performed at Argonne. Tentatively, the results appear encouraging for design purposes.

5. Shielding

Shielding studies are continuing in order to evaluate operational limitations of the plant and to develop material and thickness specifications

ultimately to be transmitted to the architect-engineer when detailed design work begins. Shielding walls surrounding the primary coolant system piping and components have been evaluated, and accessibility to various portions of the plant have been compared with operational requirements.

A preliminary cost study was made to assess the desirability of using ferrophosphorus in place of magnetite as aggregate in heavy shielding concrete. Ferrophosphorus aggregate density ranges from 5.8 to 6.3 gm/cc. The cost is 3 to 5 times the 1956 quoted prices for 4.5-gm/cc magnetite ore in carload lots. Hence, it appears magnetite remains the more economical shielding aggregate, except perhaps in specific areas where space is at a particular premium.

B. Magnetohydrodynamics (MHD)

1. MHD Generator and Cycle

The experimental work on an MHD generator with single-phase and two-phase flows was completed in October. The data have been analyzed and compared with Hartmann flow. The data in the two cases differ in that the Hartmann flow is the case for two infinite parallel planes, without end losses. In the present experiment, the channel aspect ratio was small, and end losses had a big effect. By including end losses, wall and electrode resistances, etc., the experimental data were quite close to the predicted values.

The work on liquid-metal MHD cycle analysis has continued. The cycle efficiencies of a two-component system (potassium-lithium) have been calculated by varying four parameters independently.

2. MHD Power Generation - Jet Pump Cycle

The low operating temperature of the injector jet pump during tests permitted the substitution of a transparent plastic body, combiner, and diffuser. This substitution made possible the observation of the interior behavior of the jet pump during operation with 130-psi steam. It was seen, during these runs, that the condensing shock is quite abrupt and that very little two-phase flow is encountered in the constricted high-velocity region (see Progress Report for October 1963, ANL-6801, p. 69). This fact indicates improved operation.

Subsequently, a new design of injector jet and combiner was made to allow a high steam inflow and velocity. The new combiner will optimize the flow and pressure-drop conditions. The parts are now being fabricated in the shop.

3. MHD Power Generation - Flashing Cycle

Experiments have continued with the rotating wheel generator (see Progress Report for October, 1963, ANL-6801, p. 69). It has been shown that three pulses can be put together to form an ac signal. A positive pulse is followed by a negative pulse which is followed by a positive pulse. By proper spacing of the copper strips on the rotating wheel, these pulses can be put together to form a fairly good ac waveform. These experiments show that if the fluid slugs in a MHD power generator can be properly spaced and well-defined in the pulsed flow generator, an ac waveform can be produced.

C. Regenerative EMF Cells

Thermally regenerative electrochemical cells which, in a closed cycle, would have the net effect of converting heat from a nuclear reactor or from some other source into electricity are being investigated. Two types of cells are being studied: (1) the lithium hydride cell and (2) bimetallic cells.

1. Lithium Hydride Cell

In the operation of a lithium hydride cell,[14] it is important to keep the cell operating temperature as low as possible in order to obtain maximum Carnot cycle efficiency. Thus, phase studies are being made in an effort to obtain information on systems that might yield cells of improved efficiency. The phase diagram of the LiH-LiCl system[15] and that of the LiH-LiBr system have been determined. The phase diagram of the LiH-LiBr system is shown in Figure 10. A eutectic melting at 495.6°C was found in the LiH-LiCl system. A lower melting eutectic (452.3°C) was found in the LiH-LiBr system. The deviations of both systems from ideal solution behavior are small.

2. Bimetallic Cells

Regenerative bimetallic cells,[16] which are in effect concentration cells without transference, have two liquid metal electrodes in contact with an electrolyte which consists of a fused salt mixture that contains only the salts of the more active metal. Lithium has been used as the more active metal in the bimetallic cells, because of the low density and small atomic size, which allows lithium to form very nonideal alloys with other, more noble metals. The low density of lithium permits the production of more

---

[14] Chemical Engineering Division Research Highlights, May 1962-April 1963, ANL-6766, pp. 113-7.

[15] Chemical Engineering Division Summary Report, January, February, March 1963, ANL-6687, p. 195.

[16] See Ref. 14, pp. 117-121.

electrical current per unit weight than that obtained with other metals; the formation of nonideal alloys gives rise to cell potentials that are substantially greater than those predicted for ideal concentration cells. Moreover, of the alkali metals, lithium is least soluble in its fused salts, thereby allowing operation of a cell containing a molten lithium anode and an electrolyte of molten lithium salts at elevated temperatures without appreciable solubility of lithium in the electrolyte. This low solubility is advantageous because a higher solubility would result, at best, in the irreversible transfer of lithium to the cathode and, in the extreme case, in an internal electrical short-circuit of the cell.

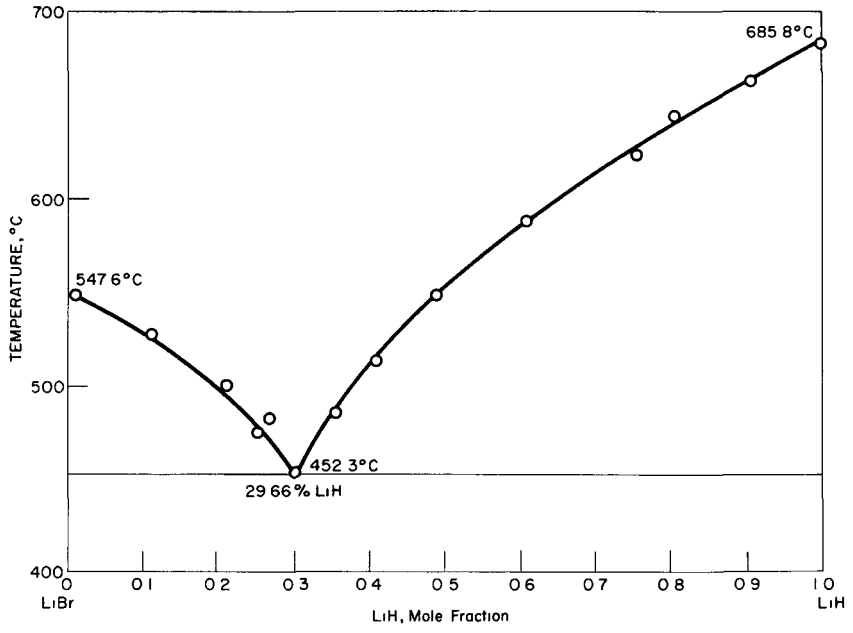

Figure 10. Phase Diagram for the LiH-LiBr System

Metals which combine with lithium to form nonideal alloys, as evidenced by the formation of intermetallic compounds whose melting points are higher than the melting point of either element, include Sn, Ga, In, Pb, Bi, Tl, Zn, Cd, and Hg. Of these combinations, the cell

$$Li(\ell)/LiCl\text{-}LiF(\ell)/Bi(\ell)$$

with X_{Li} the atom fraction of lithium, was the first to be investigated.

In operation of this cell, the normal procedure was to contain either or both electrodes in porous BeO cups which dipped into the molten electrolyte. The cell was operated in a furnace well which was connected to a dry box that contained a helium atmosphere of high purity. The atom fraction of bismuth in the cathode ranged from 0.40 to 0.95. At the lower concentrations of bismuth in the cathode, solid Li_3Bi was present as a separate phase. The cell potential was measured for each composition at various temperatures between 800 and 1080°K. The data are shown in Figure 11.

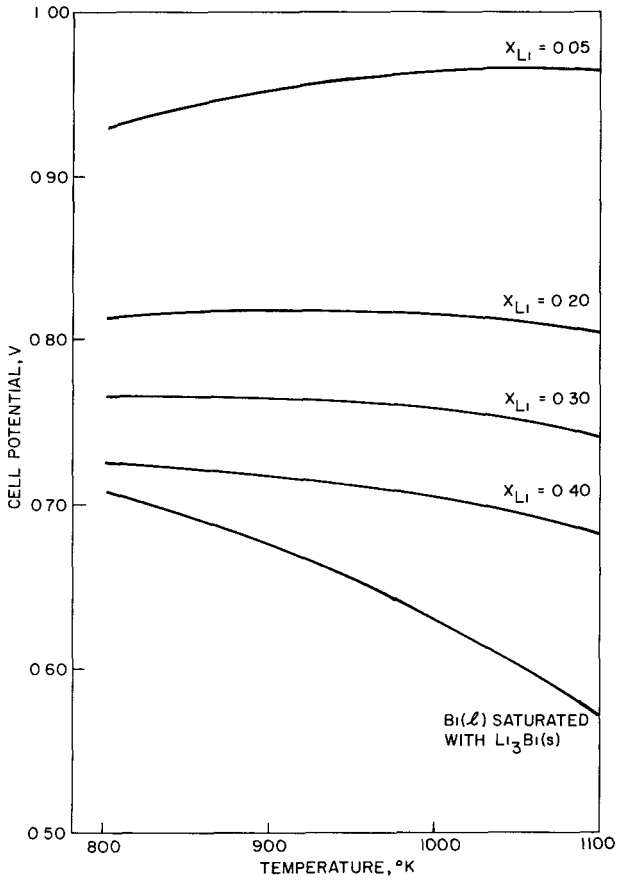

Figure 11
Cell Potential as a Function of Temperature and Cathode Composition.
Li(ℓ)/LiCl-LiF(ℓ)/Bi(ℓ) with X_{Li} the Atom Fraction of Lithium

A generalized least-squares fit of the excess chemical potential of lithium was made by means of the empirical formula

$$\Delta\mu^{E}_{Li} = A + BX_{Li},$$

where A and B are quadratic functions of temperature alone. Other partial molar thermodynamic properties of lithium were calculated directly from this expression; the Gibbs-Duhem relationship was used to calculate the partial molar thermodynamic properties of bismuth. The excess chemical potentials of lithium and bismuth are shown in Figure 12 for a cell temperature of 850°K. It should be noted that at this temperature the liquid alloy becomes saturated with solid Li_3Bi at 0.46 atom fraction lithium, and no extrapolation beyond this concentration is justified.

When the cathode is saturated with Li_3Bi, the cell reaction may be written as

$$Li(\ell) + 1/3\ Bi\ (\text{in cathode alloy}) \rightleftarrows 1/3\ Li_3Bi(s).$$

Thus, using the cell potential and the calculated value for the activity of bismuth in the cathode alloy, the standard free energy of formation of Li_3Bi(s) may be calculated and is shown as a function of temperature in Figure 13.

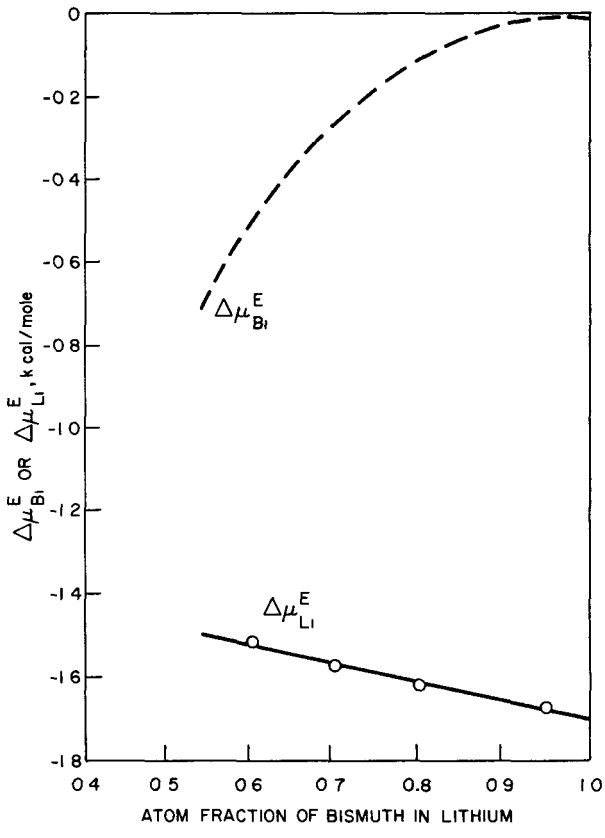

Figure 12

The Excess Chemical Potential of the Lithium-Bismuth System at 850°K

- o — Calculated directly from experimental emf data
- ——— Least-squares fit of lithium data to the equation $\Delta\mu^E_{Li} = A + BX_{Li}$
- – – – Calculated from Gibbs-Duhem relationship

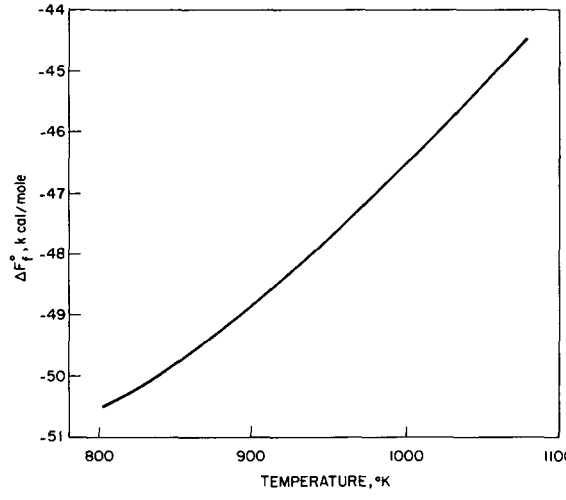

Figure 13. The Standard Free Energy of Formation of $Li_3Bi(s)$

Through use of the calculated partial molar thermodynamic properties for lithium and bismuth, it is possible to make an estimate of the vapor pressure of lithium over the alloy at higher temperatures. This estimate shows that the partial pressure of lithium over a 0.60 atom fraction lithium alloy with bismuth at 1273°K would be 0.24 mm Hg, while the partial pressure of bismuth would be 0.15 mm Hg. This indicates that the vapor pressure of lithium is so low that the separation of a large amount of lithium from the alloy would be difficult; further, the vapor would contain substantial amounts of bismuth. These facts are a direct reflection of the high cell potential expected by an extrapolation of the data in Figure 11. Thus, the relatively high cell potential that is desirable leads to a marginal regeneration of a temperature which current reactor technology cannot attain.

These considerations suggest that a system which has a slightly weaker interaction between the alkali metal and the solvent metal is more

desirable and that a slightly lower cell potential must be tolerated (or a cell with a larger temperature coefficient of potential must be found).

Two bimetallic systems, which may prove to be easier to regenerate, are being investigated. One is the lithium-tin system, which not only has a large nonideal character, but which, owing to the higher boiling point of tin as compared with that of bismuth (3003°K as compared with 1852°K), should permit a clean separation of lithium vapor from the alloy at high temperatures.

The other system which is being studied is the sodium-bismuth system. Owing to the lower boiling point of sodium, separation of a relatively pure sodium vapor from the alloy may be accomplished at temperatures attainable in present-day reactors. However, increased solubility of sodium in the electrolyte and lower cell potential as a result of less nonideal alloy formation are factors which need further investigation.

3. Regeneration of Bimetallic Cells

The simplest and probably the most practical means of regenerating a bimetallic cell is the direct thermal method. In this method the regeneration depends upon the thermal decomposition of the cathodic binary alloy product and the separation of the two components by distilling off the anodic component, which is collected at the cell operating temperature.

Exploratory experiments were carried out to assess semiquantitatively the degree of regeneration which might be expected in the alkali metal-tin system. In these experiments, alloy samples of 50-50 m/o Li-Sn and 50-50 m/o Na-Sn were placed in separate tubes which were subjected to a thermal gradient in which the temperatures at the extremities of the tubes were 950°C and 550°C. Each alloy was initially located in the hotter portion of the tube. After heating, the tubes were quenched and opened. In both tests, appreciable quantities of alkali metal had condensed in the cooler regions of the two tubes. In the test with Na-Sn alloy, 90% of the sodium originally introduced as alloy was condensed at the cooler end of the tube. The concentration of tin in sodium was found to be 40 ppm by spectrographic analysis. In the test with the Li-Sn alloy, 16.7% of the lithium metal was separated from the alloy.

V. NUCLEAR SAFETY

A. Thermal Reactor Safety Studies

1. Metal Oxidation and Ignition Studies

a. Burning-curve Ignition Studies of Uranium, Plutonium, and Their Alloys. Alloys of uranium and plutonium at an atomic ratio of about 2:1 are desired for zero-power critical experiments. Binary alloys of uranium and plutonium of this composition, however, have a tendency to crumble owing to the formation of the zeta phase (U-Pu). As a result of this crumbling tendency and the concomitant pyrophoricity of binary alloys having this atomic ratio, or one near it, work with these alloys involves excessive hazards. A study of ternary alloys was undertaken in an effort to find an alloy of suitable composition and less hazardous properties for the critical experiments.

Ignition studies were conducted with ternary alloys having atomic ratios of uranium to plutonium of about 2 to 1 with about 6 a/o of a third component present. Alloys* of uranium and plutonium with aluminum, copper, carbon, zirconium, molybdenum, or zirconium were investigated.

The burning-curve method[17] was used in these studies. In this method the temperature of the alloy is measured as the alloy is heated at a uniform rate (10°C min^{-1}) in a flowing stream of oxidant (in the present series dry air flowing at a rate of 1200 cm^3 min^{-1} was used). As the rate of the oxidation increases, the sample self-heats and finally ignites. The temperature at which the sample ignites is determined by a graphical method.

The results of the experiments are given in Table XX. The results indicate that the ternary alloys of uranium and plutonium with aluminum and copper showed little improvement over the alloy containing only uranium and plutonium. Both the carbon and zirconium alloys showed considerable self-heating between 250 and about 550°C. The ternary alloys containing iron and molybdenum, however, showed promise. The molybdenum alloy ignited at 603°C; the iron alloy did not ignite although heating was continued to 820°C. Both of these alloys showed some self-heating in

*The ternary alloys and the uranium-plutonium alloy used for comparison in the ignition studies were prepared by the Metallurgy Division (see Progress Report for September 1963, ANL-6784, p. 13).

[17] Chemical Engineering Division Summary Report April, May, June 1961, ANL-6379, p. 192.

the range from 300 to 450°C. The degree of self-heating was somewhat greater than that which occurs with pure plutonium. The nature of the self-heating suggests that specimens having higher specific areas than those of the samples tested might undergo ignition in this range; this, however, has not yet been confirmed experimentally.

Table XX. Ignition Characteristics of Uranium, Plutonium, and Their Alloys

(Burning-curve method used with 6-mm-diameter by 6-mm-long right cylinders heated in stream of dry air at rate of 10°C min^{-1})

Alloy[a]	Ignition Temp (°C)	Maximum Burning Temp (°C)
U	716	1400
Pu	524	990
U-Pu	157	820
U-Pu-Al	213	770
U-Pu-Cu	211	890
U-Pu-C	674[b]	905
U-Pu-Mo	603	950
U-Pu-Zr	no ignition to 820[c]	
U-Pu-Fe	no ignition to 820[d]	

[a]Atomic ratio of uranium to plutonium in the binary alloy was 2 to 1. Composition of the ternary alloys was about 30 a/o Pu, 6 a/o Al, Cu, C, Mo, Zr, or Fe, remainder uranium. (The alloys were prepared by the Metallurgy Division.)

[b]Self-heating from 250 to 550°C.

[c]Self-heating from 250 to 500°C.

[d]Slight self-heating from 350 to 450°C.

b. Aluminum-U_3O_8 Reaction. Studies of the aluminum-U_3O_8 thermite reaction were continued. The re-examination of this reaction was prompted by a publication[18] in which it was reported that a thermite reaction occurred in aluminum-U_3O_8 cermets. Experiments were carried out at Argonne in which cold-pressed compacts of aluminum with 30, 45, 60, 75, and 90 w/o U_3O_8 were used (see Progress Report for July 1963, ANL-6764, p. 65). The samples were subjected to two modes of heating

[18]J. D. Fleming and J. W. Johnson, Nucleonics 21(5), 84 (1963).

(see Progress Report for August 1963, ANL-6780, p. 55). In one series of tests, the samples were heated uniformly at 25°C min^{-1} to 1300°C. In the other series, the samples were heated rapidly, so that the temperature reached 1300°C in 3 to 4 min. Although some self-heating of the samples occurred in both series of experiments, the maximum self-heating recorded was at 400°C. Greatest self-heating occurred with samples containing 60 and 75 w/o U_3O_8.

Results of chemical analyses of residues from these experiments indicate the following stoichiometry:

$$U_3O_8 + 43/3\ Al \rightarrow 8/3\ Al_2O_3 + 3\ UAl_3 \quad .$$

The stoichiometric concentration of U_3O_8 in the U_3O_8-Al mixture corresponds to 68.5 w/o U_3O_8. Thus in these studies, the mixtures which contained 30, 45, and 60 w/o U_3O_8 had an excess of aluminum. In the tests with the 30 and 45 w/o U_3O_8 mixtures, more than 99% of the U_3O_8 was reacted. In tests with 60 w/o U_3O_8 mixtures, the extent of reaction ranged from 96 to 99%. In experiments with the 75 w/o U_3O_8 specimens, which contained an excess of U_3O_8, results of analyses of the metallic phases showed the overall aluminum-to-uranium ratio to be from 2.6 to 3.1 and suggested that UAl_3 is the thermodynamically favored product of the reaction. The residue from the 90 w/o U_3O_8 specimen was a hard, refractory material which was not amenable to analysis by the method used (see Progress Report for July 1963, ANL-6764, p. 65).

2. Metal-Water Reactions

a. Laser-beam Heating Applications. Research is continuing on the application of laser-beam heating to metal-water reactions. Preliminary experiments have been performed with particles of zirconium, aluminum, stainless steel, and uranium. The particle was submerged in water in a closed cell and was heated by focusing a laser beam on the particle. The extent of reaction was calculated by determining the amount of hydrogen evolved. The results of these scouting experiments have not been reproducible; for example, the extent of the zirconium-water reaction varied from 0.8 to 29%. In most tests, it was found that the particles had not been uniformly melted; some portions of the particle appeared to be destroyed, others appeared to be unaffected by the laser beam.

b. Meltdown Dynamics by the Condenser-discharge Method. The dynamics of meltdown are being studied by means of the condenser-discharge method.[19] These studies are being undertaken in an attempt to scale-up similar studies in which laser-beam heating and single particles are being used. In the present condenser-discharge tests, zirconium and platinum wires (of 30-mil diameter by 1 in. long) were heated nearly

[19] See Ref. 17, p. 200.

instantaneously to high temperature while submerged in water in a 2-ft-long channel having a cross section of 1 in. by $\frac{1}{4}$ in. The height of the water in the channel was 15 or 60 cm. The energies imparted to the wires varied from 146 to 339 cal g^{-1} in the case of zirconium and from 73 to 230 cal g^{-1} in the case of platinum. The temperatures attained by the zirconium wires ranged from 1850°C (mp) to 3500°C, and the temperatures reached by the platinum wires ranged from 1770°C (mp) to 4100°C.

In tests with zirconium wires, a void, caused by the rapid formation of hydrogen, appeared to form around the particles that were produced as a result of the electrical discharge. The production of the hydrogen resulted in a rapid movement of the water in the column. In the more energetic tests, some of the water was expelled from the column. No such voids were observed in tests with the chemically inert platinum wire. It is hoped that the tests with reactive and chemically inert substances will allow the determination of the parameters necessary to achieve oscillation of a water column. The effect of oscillation on the metal-water reaction and on the transient heat transfer will then be studied.

B. Fast Reactor Safety Studies

One of the most important design features affecting the safety of fast power reactors is the large amount of fuel required, an amount sufficient so that if the core were rearranged compactly enough a super-prompt-critical assembly would result. Therefore, one can postulate a class of "meltdown" accidents consisting, in principle, of three stages: (1) some operating abnormality in which the fuel undergoes failure (or "meltdown"); (2) the core re-forms into a more reactive configuration; (3) a destructive burst of nuclear energy occurs, terminating the incident. The mechanisms influencing failure and material movement are complex and not well understood. They are being studied in a program centering on experiments being performed in the TREAT reactor.

1. In-pile Experiments on Meltdown of Pre-irradiated Metallic Elements

A continuing program is being conducted in TREAT to study the effects of fission product accumulation on fuel-meltdown mechanism. The first four pre-irradiated specimens have been run in transparent capsules (see Monthly Report for September 1963, ANL-6784, p. 65) and are awaiting postmortem inspection and analysis. TREAT irradiation conditions are summarized in Table XXI.

The high-speed films taken during the exposure indicate that the end results of these four experiments are consistent with results obtained with previous pre-irradiated samples tested to failure in opaque capsules. Samples 1 and 2 showed the occurrence of one or more preliminary failures which are indicated by the release of small amounts of opaque vapor

(presumed to be sodium escaping from the internal bond between fuel and cladding); the large failure appeared with the characteristic high-speed release of sodium. Unirradiated specimens previously tested and photographed have not shown the multiple failures. Sample 3 received an energy input in the range between one initiating failure of fuel by swelling and clad splitting and one producing incipient fuel movement with solidified blobs of fuel attached to the cladding. Sample 3 gave an intermediate appearance between these two modes of behavior, with apparently no time delay occurring between the power transient and swelling. Upon failure, a thin opaque vapor appeared to be expelled from the sample; its origin is not known. Sample 4 produced appreciably more vapor when it failed; however, fuel movement was not completely obscured, and fuel could be seen moving in discrete particles, with evidence for expulsion from the cladding by internal pressure.

Table XXI. TREAT Exposure of Pre-irradiated Samples

Sample	Approx Burnup (a/o)	TREAT Transient Energy Release (Mw-sec)	Remarks
1. EBR-II	1	76	Extensive failure.
2. EBR-II	1	95	Extensive failure.
3. Fermi-A	0.3	35	Failure, but no disintegration.
4. Fermi-A	0.3	56	Extensive failure and fuel movement.

2. Niobium-clad Samples of Uranium Carbide

An order for 42 niobium-clad uranium carbide fuel elements has been completed by the vendor and is being prepared for shipment to ANL. The elements are of an advanced design intended for application in high-temperature, high-power density, liquid metal-cooled reactors. The fuel is 10% enriched, based on requirements for both steady-state irradiations and transient irradiations in TREAT. The uranium carbide fuel pellets, used in fabricating the elements, were pressed and sintered to approximately 90% density and are 0.648 cm in diameter. The elements are clad with 0.030-cm-thick niobium tubing and the fuel element length is 27.9 cm.

VI. PUBLICATIONS

Papers

FLUORINE BOMB CALORIMETRY. VII. THE HEAT OF FORMATION OF CADMIUM DIFLUORIDE
Edgars Rudzitis, H. M. Feder, and W. N. Hubbard
J. Phys. Chem. 67, 2388-2390 (November 1963)

NEUTRON DETECTION WITH AN ABSOLUTE FISSION COUNTER
F. S. Kirn
Neutron Dosimetry. Proc. IAEA Symp. on Neutron Detection, Dosimetry and Standardization, Harwell, December 10-14, 1962. Intern. Atomic Energy Agency, Vienna, 1963. pp. 497-512

PREPARATION AND PROPERTIES OF PLUTONIUM PHOSPHIDE (PuP)
J. B. Moser and O. L. Kruger
Ceramic News XII(10), 61 (October 1963)

SINTERING STUDIES ON PLUTONIUM MONOCARBIDE
O. L. Kruger
Ceramic News XII(10), 61 (October 1963)

NEUTRON RADIOGRAPHY - A NEW DIMENSION IN RADIOGRAPHY
Harold Berger
Nondestructive Testing 21, 369-373 (November-December 1963)

ELECTRONIC INTEGRATOR FOR USE WITH A DIFFERENTIAL CALORIMETER
J. J. Eichholz and J. B. Darby, Jr.
Rev. Sci. Instr. 34(11), 1274-1275 (November 1963)

INTERACTION OF HEAT TRANSFER BY CONDUCTION, CONVECTION AND RADIATION IN A RADIATING FLUID
Raymond Viskanta
J. Heat Transfer 85(4), 318-328 (1963)

FREE CONVECTIVE HEAT TRANSFER TO SUPERCRITICAL WATER EXPERIMENTAL MEASUREMENTS
C. A. Fritsch and R. J. Grosh
J. Heat Transfer 85(4), 289-294 (1963)

A MONITORING TECHNIQUE FOR RADIATION DAMAGE EXPERIMENTS
A. D. Rossin
Neutron Dosimetry. Proc. IAEA Symp. on Neutron Detection, Dosimetry and Standardization, Harwell, December 10-14, 1962. Intern. Atomic Energy Agency, Vienna, 1963. pp. 515-520

FAST NEUTRON DOSIMETRY FOR RADIATION DAMAGE STUDIES
A. D. Rossin and R. J. Armani
Neutron Dosimetry. Proc. IAEA Symp. on Neutron Detection, Dosimetry and Standardization, Harwell, December 10-14, 1962. Intern. Atomic Energy Agency, Vienna, 1963. pp. 293-304

SIGNIFICANCE OF NEUTRON SPECTRUM ON RADIATION EFFECTS STUDIES
A. D. Rossin
Proc. Symp. on Radiation Effects on Metals and Neutron Dosimetry, Los Angeles, October 2-3, 1962. A.S.T.M., Philadelphia, 1963, pp. 115-132

ALGORITHM 215. SHANKS
H. C. Thacher, Jr.
Commun. Assoc. Computing Mach. 6(11), 662 (November 1963)

CERTIFICATION OF ALGORITHM 8. EULER SUMMATION
H. C. Thacher, Jr.
Commun. Assoc. Computing Mach. 6(11), 663 (November 1963)

NUMERICAL INTEGRATION AND DIFFERENTIATION OF FUNCTIONS OF SEVERAL INDEPENDENT VARIABLES BY AN ITERATIVE PROCEDURE
H. C. Thacher, Jr.
J. Soc. Ind. Appl. Math. 11(3), 614-622 (September 1963)

GAMMA-RAY DISCRIMINATION ON A PROTON-RECOIL PROPORTIONAL COUNTER
E. F. Bennett
Neutron Dosimetry. Proc. IAEA Symp. on Neutron Detection, Dosimetry and Standardization, Harwell, December 10-14, 1962. Intern. Atomic Energy Agency, Vienna, 1963. pp. 341-346

PRECISION LIMITATIONS IN THE MEASUREMENT OF SMALL REACTIVITY CHANGES
E. F. Bennett and R. L. Long
Nucl. Sci. Eng. 17, 425-432 (November 1963)

Transactions of the American Nuclear Society, 6(2), (November 1963)

EBWR TRANSFER FUNCTIONS
W. C. Lipinski, C. Hsu, G. F. Popper, and A. Hirsch, p. 209

CRITICAL EXPERIMENT WITH BORAX-V SUPERHEATER ELEMENTS
K. E. Plumlee, Q. L. Baird, G. S. Stanford, and P. I. Amundson
p. 217

BEHAVIOR OF IRRADIATED METALLIC FUEL ELEMENTS EXPOSED TO NUCLEAR EXCURSIONS IN TREAT
J. H. Monaweck, C. E. Dickerman, and E. S. Sowa
pp. 374-375

DEGRADATION OF IMPACT ENERGY OF STEEL AS A FUNCTION OF NEUTRON EXPOSURE
A. D. Rossin
pp. 389-390

POSTIRRADIATION EVALUATION OF EBR-I MARK III FUEL RODS
Richard Carlander and F. D. McGinnis
p. 373

SWELLING OF CAST THORIUM/URANIUM ALLOYS DURING IRRADIATION AND POSTIRRADIATION ANNEALING
J. H. Kittel, C. F. Reinke, and J. A. Horak
p. 372

MATERIALS FOR ARGONNE NATIONAL LABORATORY SODIUM-COOLED REACTORS
R. E. Macherey, W. R. Simmons, and R. A. Noland
p. 360

POWER MAPPING IN BORAX-V BOILING CORE B-2 BY FUEL ROD ACTIVATION
R. A. Cushman
p. 218

THE DETERMINATION OF Pu^{239} PRODUCTION PATTERNS IN EBR-I
R. R. Smith, R. O. Haroldsen, and R. E. Horne
p. 423

THE IRRADIATION BEHAVIOR OF URANIUM MONOSULFIDE
L. A. Neimark and P. D. Shalek
p. 372

ESTABLISHING AND MAINTAINING A HIGH-PURITY INERT ATMOSPHERE IN EBR-II FUEL CYCLE FACILITY ARGON CELL
J. H. Schraidt, L. F. Coleman, Milton Levenson, J. O. Ludlow, and W. F. Holcomb
Trans. Am. Nucl. Soc. 6(2), 454 (November 1963). Proc. 11th Conf. on Hot Laboratories and Equipment, New York, November 18-21, 1963. Am. Nucl. Soc., Hinsdale, Ill., 1963, pp. 181-190.

INTRODUCTORY REMARKS: REMOTE HANDLING OPERATIONS FOR DEVELOPMENT TESTING OF NUCLEAR ROCKETS

M. J. Feldman

Trans. Am. Nucl. Soc. 6(2), 448 (November 1963). Proc. 11th Conf. on Hot Laboratories and Equipment, New York, November 18-21, 1963. Am. Nucl. Soc., Hinsdale, Ill., 1963, pp. 175-176.

A SIMPLIFIED PROCEDURE FOR ALTERATION AND MAINTENANCE OF PLUTONIUM

H. V. Rhude and L. R. Kelman

Trans. Am. Nucl. Soc. 6(2), 461 (November 1963). Proc. 11th Conf. on Hot Laboratories and Equipment, New York, November 18-21, 1963. Am. Nucl. Soc., Hinsdale, Ill., 1963, pp. 347-351.

ARGONNE PHYSICAL AND METALLURGICAL HOT LABORATORY

W. B. Doe

Trans. Am. Nucl. Soc. 6(2), 473 (November 1963). Proc. 11th Conf. on Hot Laboratories and Equipment, New York, November 18-21, 1963. Am. Nucl. Soc., Hinsdale, Ill., 1963, pp. 460-461.

THE FRACTURE BY ELECTRICAL DISCHARGE OF GAMMA-IRRADIATED SHIELDING WINDOW GLASS

F. C. Hardtke and K. R. Ferguson

Trans. Am. Nucl. Soc. 6(2), 463 (November 1963). Proc. 11th Conf. on Hot Laboratories and Equipment, New York, November 18-21, 1963. Am. Nucl. Soc., Hinsdale, Ill., 1963. pp. 369-381.

PROBLEMS ASSOCIATED WITH THE USE OF INFLATABLE SEALS FOR ENCLOSURES CONTAINING HIGH-PURITY ATMOSPHERES

D. P. Mingesz and D. E. Czernik

Trans. Am. Nucl. Soc. 6(2), 463 (November 1963). Proc. 11th Conf. on Hot Laboratories and Equipment, New York, November 18-21, 1963. Am. Nucl. Soc., Hinsdale, Ill., 1963. pp. 361-368.

THE ESTIMATION OF GAMMA-RAY SHIELDING FOR HOT CELLS

K. R. Ferguson

Proc. 11th Conf. on Hot Laboratories and Equipment, New York, November 18-21, 1963. Am. Nucl. Soc., Hinsdale, Ill., 1963. pp. 469-475.

ANL Reports

ANL-6504 SAFETY ANALYSIS OF PLUTONIUM LOADINGS IN ZPR-III [Addendum to ANL-6408, Hazard Evaluation Report on the Fast Reactor Zero Power Experiment (ZPR-III)]
J. K. Long

ANL-6671 DENSITY MEASUREMENTS IN GLOVEBOXES. With Density Data on Monobromobenzene, Cast Thorium, Thorium-Uranium, and Thorium-Plutonium Alloys
B. Blumenthal

ANL-6681 A SURVEY OF PROMPT-NEUTRON LIFETIMES IN FAST CRITICAL SYSTEMS
G. S. Brunson, R. N. Curran, J. M. Gasidlo, and R. J. Huber

ANL-6684 THE MECHANISM AND KINETICS OF THE REACTION BETWEEN NICKEL AND FLUORINE
R. L. Jarry, W. H. Gunther, and J. Fischer

ANL-6687 CHEMICAL ENGINEERING DIVISION SUMMARY REPORT, January, February, March, 1963

ANL-6742 LABORATORY INVESTIGATIONS IN SUPPORT OF FLUID BED FLUORIDE VOLATILITY PROCESSES. Part I. The Fluorination of Uranium Dioxide-Plutonium Dioxide Solid Solutions
R. L. Jarry, L. J. Anastasia, J. Fischer, L. E. Trevorrow, T. D. Baker, and J. J. Stockbar

ANL-6753 LABORATORY INVESTIGATIONS IN SUPPORT OF FLUID BED FLUORIDE VOLATILITY PROCESSES. Part II. The Properties of Plutonium Hexafluoride
Martin J. Steindler

ANL-6758 NUCLEAR THERMIONIC CONVERTERS FOR SPACE POWER
J. C. Carter, A. J. Ulrich, and R. H. Armstrong (Classified)

ANL-6762 LABORATORY INVESTIGATIONS IN SUPPORT OF FLUID BED FLUORIDE VOLATILITY PROCESSES. Part III. Separation of Gaseous Mixtures of Uranium Hexafluoride and Plutonium Hexafluoride by Thermal Decomposition
L. Trevorrow, J. Fischer, and J. Riha

ANL-6774 NUCLEAR ROCKET STUDY EVALUATION REPORT
J. F. Marchaterre, K. K. Almenas, G. H. Golden, B. M. Hoglund, V. M. Kolba, and W. Loewenstein
(Classified)